

DOI: 10.1002/cmdc.201400058

Development of 3-Phenyl-*N*-(2-(3-phenylureido)ethyl)-thiophene-2-sulfonamide Compounds as Inhibitors of Antiapoptotic Bcl-2 Family Proteins

Chengwen Yang,^[a] Sha Chen,^[b] Mi Zhou,^[a] Yan Li,^[a] Yangfeng Li,^[a] Zhengxi Zhang,^[a] Zhen Liu,^[a] Qian Ba,^[c] Jingquan Li,^[c] Hui Wang,^[c] Xiaomei Yan,^{*,[b]} Dawei Ma,^{*,[a]} and Renxiao Wang^{*,[a]}

Antiapoptotic Bcl-2 family proteins, such as Bcl-x_L, Bcl-2, and Mcl-1, are often overexpressed in tumor cells, which contributes to tumor cell resistance to chemotherapies and radiotherapies. Inhibitors of these proteins thus have potential applications in cancer treatment. We discovered, through structure-based virtual screening, a lead compound with micromolar binding affinity to Mcl-1 (inhibition constant (*K*) = 3 μM). It contains a phenyltetrazole and a hydrazinecarbothioamide moiety, and it represents a structural scaffold not observed among known Bcl-2 inhibitors. This work presents the structural optimization of this lead compound. By following the scaffold-hopping strategy, we have designed and synthesized a total of 82 compounds in three sets. All of the compounds were evaluated in a fluorescence-polarization binding assay to measure their binding affinities to Bcl-x_L, Bcl-2, and Mcl-1.

Some of the compounds with a 3-phenylthiophene-2-sulfonamide core moiety showed sub-micromolar binding affinities to Mcl-1 (*K*_i = 0.3–0.4 μM) or Bcl-2 (*K*_i ≈ 1 μM). They also showed obvious cytotoxicity on tumor cells (IC₅₀ < 10 μM). Two-dimensional heteronuclear single quantum coherence NMR spectra of three selected compounds, that is, YCW-E5, YCW-E10, and YCW-E11, indicated that they bind to the BH3-binding groove on Bcl-x_L in a similar mode to ABT-737. Several apoptotic assays conducted on HL-60 cells demonstrated that these compounds are able to induce cell apoptosis through the mitochondrial pathway. We propose that the compounds with the 3-phenylthiophene-2-sulfonamide core moiety are worth further optimization as effective apoptosis inducers with an interesting selectivity towards Mcl-1 and Bcl-2.

Introduction

Apoptosis, or programmed cell death, is an essential physiological process required for the development and maintenance of tissue homeostasis. Deregulation of this process is known to be associated with various types of cancer.^[1–5] The B-cell lymphoma 2 (Bcl-2) family of proteins is a major group of apoptosis regulators, which includes both antiapoptotic members

(such as Bcl-2, Bcl-x_L, Mcl-1, and Bcl-w), proapoptotic members (such as Bak and Bax), and BH3-only proteins.^[6] Overexpression of antiapoptotic Bcl-2 family proteins contributes to resistance to chemotherapies and radiotherapies in many tumor cells. Hence, the Bcl-2 family of proteins has become an attractive molecular target for the development of new cancer therapies since the beginning of this century.^[7,8]

The antiapoptotic members in the Bcl-2 family conduct their biological functions through protein–protein interactions with the proapoptotic members.^[6] Designing small-molecule inhibitors of protein–protein interactions has been considered as reaching for the high-hanging fruits in drug discovery.^[9–11] Despite the challenge, a number of small-molecule inhibitors of Bcl-2 family proteins have been publicly reported in the past ten years or so,^[12–34] which makes the Bcl-2 family proteins perhaps the most popular targets in this category. Some of the best-known Bcl-2 family protein inhibitors are summarized in Figure 1. A few of them have successfully entered phase II clinical trials, such as Navitoclax (ABT-263) developed by Abbott Laboratories.^[12–14] But no small-molecule compound has entered phase III trials so far. Despite all of the progress, Bcl-2 inhibitors are still very limited as compared with other well-established drugs. In particular, novel chemical scaffolds are de-

[a] Dr. C. Yang, M. Zhou, Dr. Y. Li, Y. Li, Z. Zhang, Dr. Z. Liu, Prof. D. Ma, Prof. R. Wang
State Key Laboratory of Bioorganic & Natural Products Chemistry
Shanghai Institute of Organic Chemistry, Chinese Academy of Sciences
345 Lingling Rd, Shanghai 200032 (P. R. China)
E-mail: madw@main.sioc.ac.cn
wangrx@mail.sioc.ac.cn

[b] S. Chen, Prof. X. Yan
MOE Key Laboratory of Spectrochemical Analysis & Instrumentation
Key Laboratory for Chemical Biology of Fujian Province
Department of Chemical Biology, College of Chemistry & Chemical Engineering, Xiamen University
422 Siming South Rd, Xiamen, Fujian 361005 (P. R. China)
E-mail: xmyan@xmu.edu.cn

[c] Dr. Q. Ba, Dr. J. Li, Prof. H. Wang
Institute of Nutritional Sciences
Shanghai Institutes of Biological Sciences, Chinese Academy of Sciences
319 Yueyang Rd, Shanghai 200031 (P. R. China)

Supporting information for this article is available on the WWW under <http://dx.doi.org/10.1002/cmdc.201400058>.

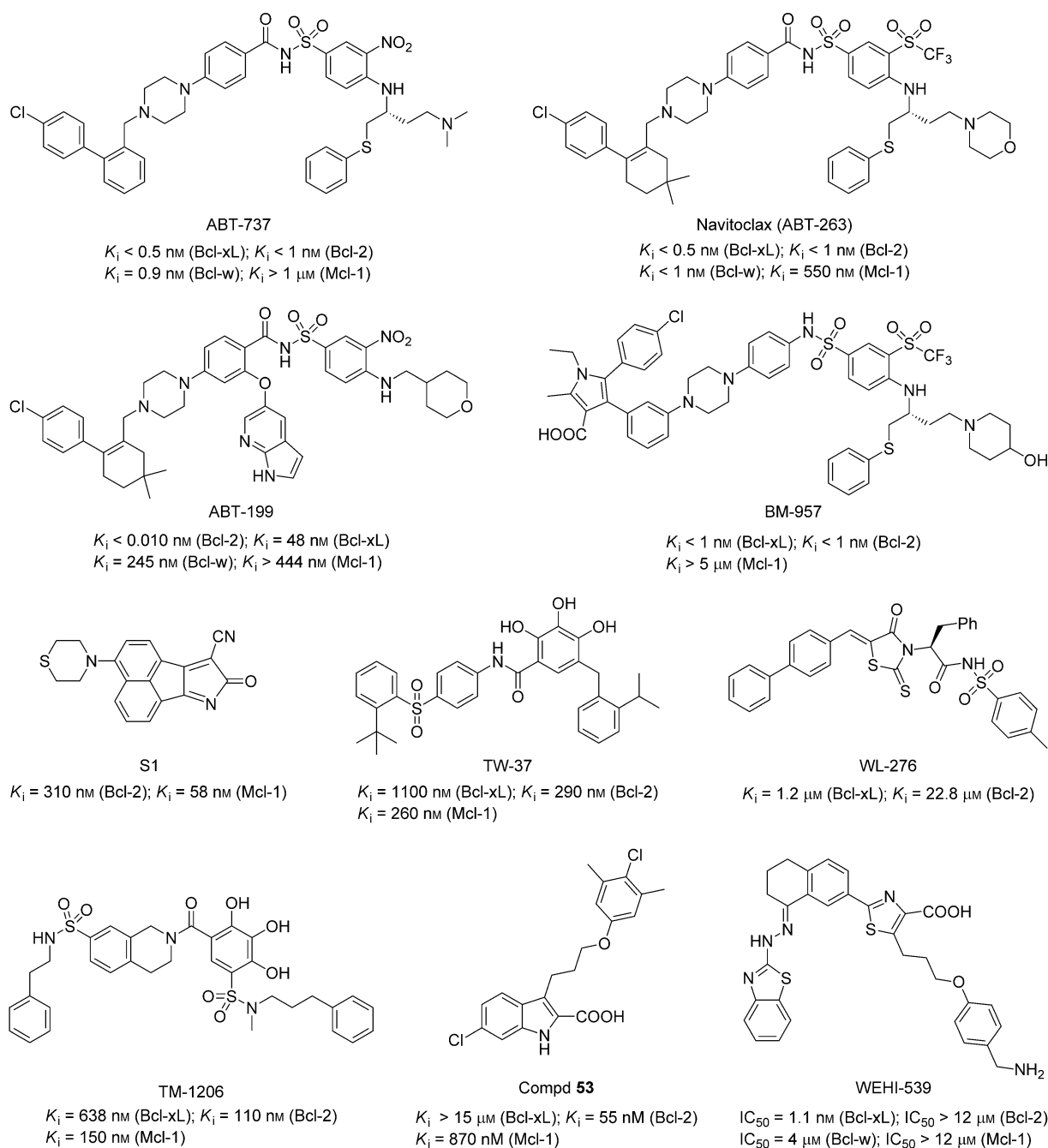


Figure 1. Some known small-molecule inhibitors of antiapoptotic Bcl-2 family proteins and their binding data reported in the literature.^[12–34]

sired to increase the chance of discovering successful drug candidates.

In addition, the selectivity of Bcl-2 inhibitors has drawn public attention recently.^[35] Although all antiapoptotic Bcl-2 family proteins have similar 3D structures, the sequence identities among them are only modest, typically around 30–70%, which implies that they may target different types of tissues in apoptosis and may also differ in responses to different stress stimuli.^[36] In fact, more selective inhibitors of certain Bcl-2 family proteins have been revealed recently. For example, Souers et al. reported the re-engineering of Navitoclax to

obtain a potent, orally available, selective inhibitor of Bcl-2, that is, ABT-199.^[30] This compound inhibits the growth of Bcl-2-dependent tumors in vivo and spares human platelets. But, so far, many Bcl-2 family inhibitors are still more potent towards Bcl-2 or Bcl-x_L than Mcl-1. For example, ABT-737 and ABT-263 were found to be highly potent inhibitors of Bcl-2, Bcl-x_L, and Bcl-w (inhibition constant (K_i) < 1 nM) but only modestly affected Mcl-1 ($K_i = 0.55$ μ M).^[12–14] They thus lack efficacy on some types of cancer cells with Mcl-1 overexpression. Indeed, down-regulation of Mcl-1 makes cancer cells sensitive to ABT-737 or other cytotoxic agents.^[37–39] Thus, inhibitors of

Mcl-1 and other less-noted antiapoptotic Bcl-2 family proteins are expected to supplement current Bcl-2/Bcl-x_L inhibitors to provide more effective or more selective cancer therapies.

In order to discover inhibitors of Bcl-2 family proteins with new chemical scaffolds, we conducted virtual screening of small-molecule compounds by targeting Mcl-1 in our previous study. Mcl-1 was chosen as the target because it has been discovered in recent years that the biological functions of Mcl-1 are notably different from those of other antiapoptotic Bcl-2 family proteins, such as Bcl-2 or Bcl-x_L. In fact, the sequence similarity between Mcl-1 and Bcl-2 is only 30%, which indicates its independent characteristics.^[35] Over 56 000 compounds from the Maybridge chemical catalogue (released in August 2008) were docked into the BH3-binding groove on Mcl-1 by using GOLD software (version 5.1). After visual examination of the top-ranked candidates suggested by molecular docking, we manually selected 200 compounds. Samples of these compounds were ordered and then tested in a fluorescence-polarization (FP)-based binding assay. Among them, one compound, BCL-VS-156 (Scheme 1), showed clear dose-dependent binding to Mcl-1 with a K_i value of 3.0 μM . Although this level of binding affinity is only modest, this compound consists of a phenyltetrazole and a hydrazinecarbothioamide moiety, which are not observed among known Bcl-2 inhibitors. By taking this compound as the lead compound, we synthesized a total of 82 derivative compounds in three sets (Scheme 1). Finally, we

obtained some compounds with a 3-phenylthiophene-2-sulfonamide core moiety that exhibited both promising binding affinities to the target proteins and cytotoxicity on tumor cells. The best compounds have sub-micromolar binding affinities to Mcl-1 and Bcl-2 and are about 10-fold more potent than the lead compound. We also demonstrated in several apoptosis assays that these compounds effectively induced cell apoptosis through the mitochondrial pathway.

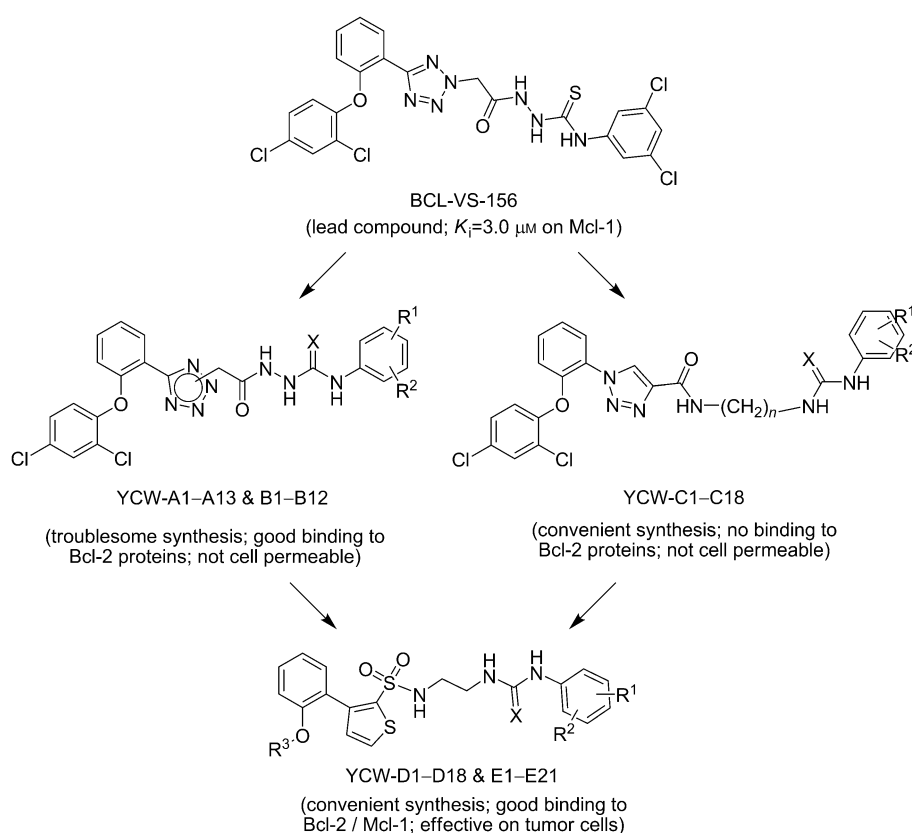
Results and Discussion

1. Hopping from the lead compound to the thiophene-2-sulfonamide compounds

In order to confirm the binding affinity of the lead compound (BCL-VS-156) to the Bcl-2 family proteins, the first set of compounds synthesized by us were direct derivatives of the lead compound, which all contain a phenyltetrazole moiety as well as a hydrazinecarbothioamide moiety (Table 1). The synthetic methods for preparing this set of compounds are outlined in Scheme 2. A pair of regioisomers, **3a** and **3b**, were actually obtained after compound **2** reacted with methyl bromoacetate. These two regioisomers were carefully separated and applied in the subsequent reactions, and two sets of compounds were thus obtained, that is, YCW-A1–A13 and YCW-B1–B12. For both sets of compounds, the phenyl rings connected to the thiourea moiety were modified with

small-size electron-donating (such as methyl and methoxy) or electron-withdrawing (such as trifluoromethyl and nitro) substituent groups. In addition, the thiourea moiety was replaced by a urea moiety. The overall yields of the A and B compounds were generally higher than 80% (with only two exceptions). However, some steps in the synthetic route were not completely practical. For example, azides were needed to introduce the tetrazole ring and some reactions required a long period of heating at reflux. The purity of most of the A compounds ranged from 90–99%. But the purifications of some of the B compounds were relatively troublesome, and the purity of six B compounds was only around 75%.

Compounds YCW-A1–A13 and YCW-B1–B12 were all tested in an FP-based binding assay, which was applied successfully in our previous studies.^[40–42] The results of our binding assay indicated that these compounds



Scheme 1. An overview of how the thiophene-2-sulfonamide compounds were derived from the lead compound in our study.

Table 1. Chemical structures and binding data for the A and B compounds.

Compd	X	A1–A13			Yield [%]	B1–B12		
		R ¹	R ²	Bcl-x _L		K _i [μM] ^[a]	Mcl-1	
YCW-A1	S	3-Me	H	86	weak	3.6 ± 0.8	5.0 ± 1.3	
YCW-A2	S	3-Cl	H	88	9.3 ± 1.9	5.2 ± 0.2	6.7 ± 2.4	
YCW-A3	S	3-MeO	H	85	weak	5.8 ± 2.0	10.6 ± 0.4	
YCW-A4	S	3-NO ₂	H	89	3.1 ± 0.6	4.1 ± 0.2	2.7 ± 0.1	
YCW-A5	S	4-Cl	H	87	weak	2.8 ± 0.2	4.3 ± 0.4	
YCW-A6	S	4-MeO	H	86	weak	10.2 ± 7.0	9.7 ± 3.7	
YCW-A7	S	4-NO ₂	H	89	3.5 ± 0.8	1.9 ± 0.4	2.2 ± 0.2	
YCW-A8	S	3-CF ₃	5-CF ₃	61	13 ± 1.2	0.80 ± 0.06	6.5 ± 4.1	
YCW-A9	O	3-Me	5-Me	85	N.A.	N.A.	N.A.	
YCW-A10	O	4-Cl	H	59	N.A.	N.A.	N.A.	
YCW-A11	O	4-MeO	H	85	N.A.	N.A.	N.A.	
YCW-A12	O	4-NO ₂	H	86	N.A.	N.A.	N.A.	
YCW-A13	O	3-Cl	5-Cl	89	N.A.	N.A.	N.A.	
YCW-B1	S	3-Me	H	88	9.5 ± 5.1	5.6 ± 1.1	6.1 ± 0.92	
YCW-B2	S	3-Cl	H	89	9.4 ± 7.1	4.3 ± 1.5	5.0 ± 1.4	
YCW-B3	S	3-MeO	H	87	5.2 ± 2.4	20 ± 6.0	5.2 ± 2.2	
YCW-B4	S	3-NO ₂	H	91	7.5 ± 1.1	2.5 ± 0.20	2.8 ± 1.5	
YCW-B5	S	4-Cl	H	89	weak	3.0 ± 0.4	4.5 ± 0.8	
YCW-B6	S	4-MeO	H	87	10 ± 7.5	7.2 ± 2.7	4.6 ± 1.3	
YCW-B7	S	4-NO ₂	H	91	3.0 ± 1.3	2.4 ± 0.1	2.0 ± 0.1	
YCW-B8	O	4-Cl	H	89	N.A.	N.A.	N.A.	
YCW-B9	O	4-MeO	H	84	N.A.	N.A.	N.A.	
YCW-B10	O	4-NO ₂	H	91	N.A.	N.A.	N.A.	
YCW-B11	O	3-Me	5-Me	88	N.A.	N.A.	N.A.	
YCW-B12	O	3-Cl	5-Cl	90	N.A.	N.A.	N.A.	

[a] The mean values and standard deviations of the K_i values were derived based on the outcomes of three parallel measurements. N.A.: No obvious sign of binding was observed; weak: dose-dependent FP signals were observed, but the change in the FP signals (up to 100 μM concentration) was not significant enough to determine the K_i value accurately.

generally have K_i values ranging between 1–20 μM for Bcl-2 and between 2–11 μM for Mcl-1. As for Bcl-x_L, some of these compounds have micromolar binding affinities, whereas the binding affinities of others were too weak to determine accurately. These results confirmed that the A and B compounds, which share the same structural scaffold as the lead compound, are able to bind to the Bcl-2 family proteins. But no compound was found to have really improved binding affinities relative to that of the lead compound. Another notable observation was that, when the thiourea moiety was replaced by a urea moiety, the resulting compounds lost their binding affinities completely.

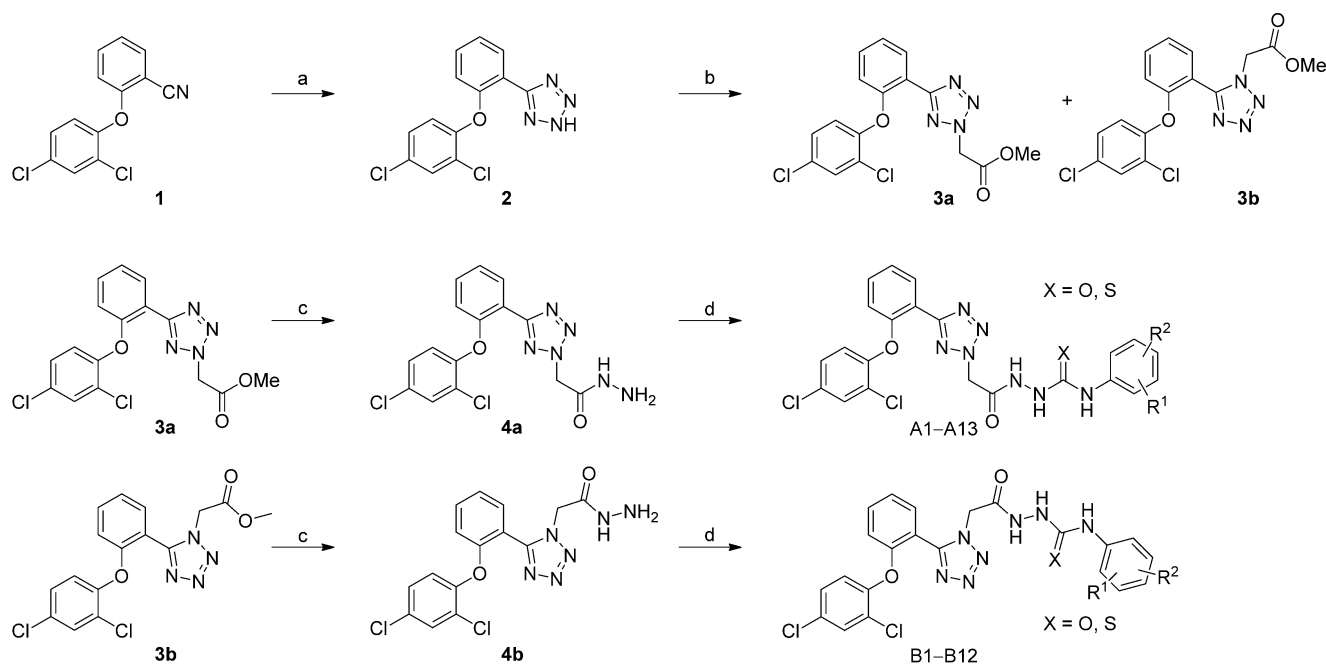
All of the A and B compounds were also screened by 3-(4,5-dimethylthiazol-2-yl)-2,5-diphenyltetrazolium bromide (MTT) viability assays on six tumor cell lines. It needs to be emphasized that the outcomes of an MTT assay should not be related directly to a certain molecular target. In our study, this assay served as a basic measure for characterizing the cell permeability and cytotoxicity of our compounds. Some of the com-

pounds were selected based on the MTT assay results, and they were tested in more sophisticated assays to explore their apoptosis-inducing mechanism. Our results showed that none of the A or B compounds exhibited obvious cytotoxicity on any cell line under test. Thus, it seems that these two sets of compounds are not very cell permeable, and they are not likely to target Bcl-2 family proteins effectively in living cells.

Due to the difficulties in organic synthesis as well as the poor cell permeability of the A and B compounds, as our next attempt, we synthesized another set of compounds by replacing the phenyltetrazole moiety with a phenyltriazole moiety (Table 2). These compounds (YCW-C1–C18) were synthesized as outlined in Scheme 3. In this case, the popular “click-chemistry”^[43] method was adopted to introduce the triazole ring. The other change in the structural scaffold was that the amide group is attached to the triazole ring directly, and it is separated from the thiourea moiety by one or two methylene units. With these changes, this set of compounds was generally more convenient to synthesize than the A and B compounds. The overall yields of most of the compounds in this set (only one exception) were over 80%, and their purities were all above 90%.

Compounds YCW-C1–C18 were also tested in our FP-based assay to measure their binding to the three antiapoptotic Bcl-2 family proteins. Unexpectedly, all of them exhibited none or very weak binding to the three target proteins. Our molecular modeling results suggested that the low-energy conformation of the C compounds is more rigid than those of the A or B compounds. As indicated by the predicted binding mode of the lead compound (Figure 2a), a certain level of conformation flexibility in the backbone is necessary for maintaining binding to Mcl-1. The rigidity is perhaps the reason why the C compounds cannot bind to the desired targets. This set of compounds were also tested on tumor cell lines in MTT assays. Most of them did not exhibit obvious cytotoxicity on tumor cell lines. Thus, this set of compounds were not further pursued in our study.

We then continued applying the scaffold-hopping strategy to develop new derivative compounds. This time, we chose the thiophene-2-sulfonamide moiety to replace the five-membered tetrazole or triazole moiety in the A/B/C compounds. Both the thiophene and sulfonamide groups are common in many drug molecules. They were chosen also because of their synthetic feasibility. As a result, a new set of compounds, that is, YCW-D1–D18 (Table 3), were synthesized as outlined in Scheme 4. In this case, the thiophene-2-sulfonamide moiety (in **16**) was prepared by sulfonylation of the available starting material **14**. Compound **16** was then connected to a phenylboronic acid derivative, **13**, **21a**, or **21b**, through the Suzuki cross-coupling reaction. The product after deprotection, **18**, **23a**, or



Scheme 2. Synthesis of compounds YCW-A1–A13 and YCW-B1–B12. *Reagents and conditions:* a) NaN_3 , $\text{Et}_3\text{N}\cdot\text{HCl}$, DMF, reflux, 2 h, 45%; b) methyl bromoacetate, NaH, THF, reflux, 5 h, 56% for **3a**, 34% for **3b**; c) $\text{N}_2\text{H}_4\cdot\text{H}_2\text{O}$, THF, reflux, 12 h, **4a**: 92%, **4b**: 91%; d) aryl isothiocyanate or aryl isocyanate, THF, reflux.

Table 2. Chemical structures for the C compounds.

Compd	R ¹	R ²	Yield [%]
YCW-C1	H	H	90
YCW-C2	3-Me	H	93
YCW-C3	3-Cl	H	88
YCW-C4	3-MeO	H	93
YCW-C5	3-NO ₂	H	89
YCW-C6	4-Cl	H	93
YCW-C7	4-MeO	H	86
YCW-C8	4-NO ₂	H	92
YCW-C9	3-CF ₃	5-CF ₃	92
YCW-C10	H	H	92
YCW-C11	3-Me	H	88
YCW-C12	3-Cl	H	86
YCW-C13	3-MeO	H	84
YCW-C14	3-NO ₂	H	91
YCW-C15	4-Cl	H	76
YCW-C16	4-MeO	H	83
YCW-C17	4-NO ₂	H	87
YCW-C18	3-CF ₃	5-CF ₃	87

23b, was connected to an aryl isothiocyanate to obtain the final compounds. With this synthetic route, the whole chemical structure of this set of compounds was dissected into three building blocks. These building blocks were prepared in a parallel manner, and combination of them yielded the final compounds with the desired structural diversity. The overall yields

Table 3. Chemical structures for the D compounds.

Compd	R ¹	R ²	R ³	Yield [%]
YCW-D1	3-Me	H	2,4-dichlorophenyl	99
YCW-D2	3-Cl	H	2,4-dichlorophenyl	98
YCW-D3	3-MeO	H	2,4-dichlorophenyl	99
YCW-D4	3-NO ₂	H	2,4-dichlorophenyl	95
YCW-D5	4-Cl	H	2,4-dichlorophenyl	99
YCW-D6	4-MeO	H	2,4-dichlorophenyl	96
YCW-D7	4-NO ₂	H	2,4-dichlorophenyl	99
YCW-D8	3-CF ₃	5-CF ₃	2,4-dichlorophenyl	97
YCW-D9	3-MeO	H	1-naphthyl	90
YCW-D10	3-NO ₂	H	1-naphthyl	95
YCW-D11	4-MeO	H	1-naphthyl	91
YCW-D12	4-NO ₂	H	1-naphthyl	93
YCW-D13	3-CF ₃	5-CF ₃	1-naphthyl	90
YCW-D14	3-MeO	H	2-naphthyl	99
YCW-D15	3-NO ₂	H	2-naphthyl	97
YCW-D16	4-MeO	H	2-naphthyl	90
YCW-D17	4-NO ₂	H	2-naphthyl	91
YCW-D18	3-CF ₃	5-CF ₃	2-naphthyl	89

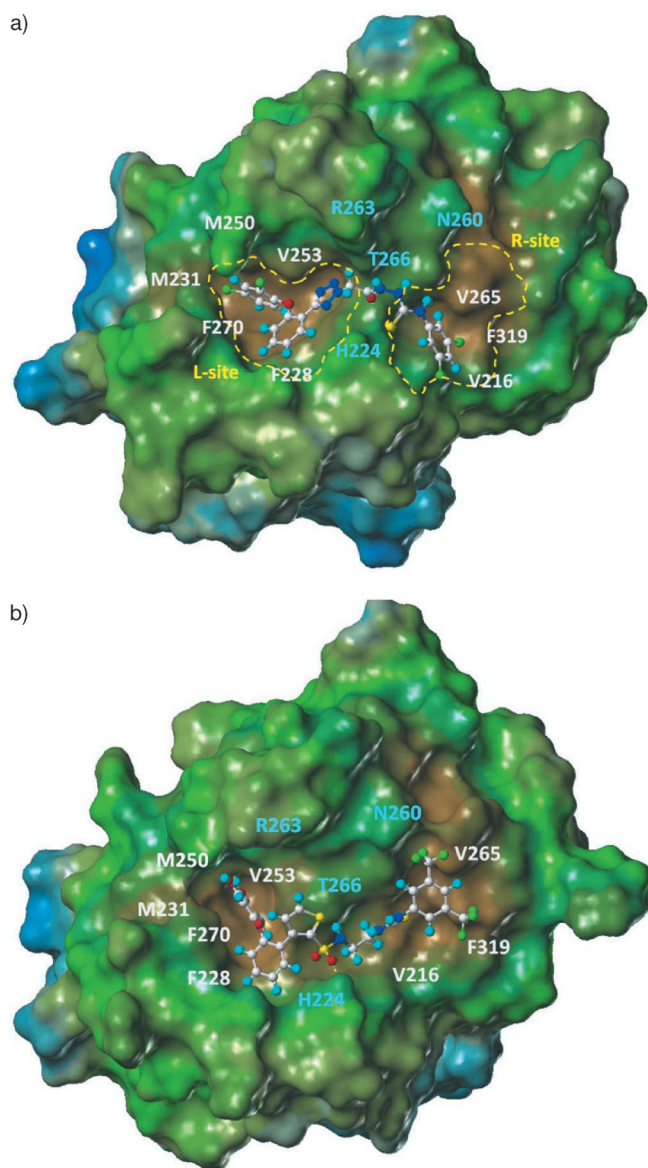


Figure 2. Binding modes of a) the lead compound BCL-VS-156 and b) one of our most potent compounds (YCW-E5) with Mcl-1, as predicted by molecular modeling. The ligand molecule is rendered as a ball-and-stick model. The molecular surface of Mcl-1 is colored on a lipophilicity scale, in which polar regions are blue and green and lipophilic regions are brown. The locations of the binding pocket residues are labeled: hydrophobic residues have white labels and polar residues have cyan labels. These pictures were prepared by using the SYBYL software. Other representations of these two binding modes are given in the Supporting Information (part II).

of most of the compounds in this set (only one exception) are over 90%, and their purities are all above 90%.

Compounds YCW-D1–D18 were then tested in our FP-based assay to measure their binding affinities with the three antiapoptotic Bcl-2 family proteins. Again, none of them exhibited obvious activity in our binding assay. But quite a few of the D compounds exhibited obvious cytotoxicity ($IC_{50} < 10 \mu\text{M}$) on tumor cell lines (Table 5), which indicated improved cell permeability of this structural scaffold relative to the A/B/C compounds described above. This observation encouraged us to explore other modifications on this structural scaffold.

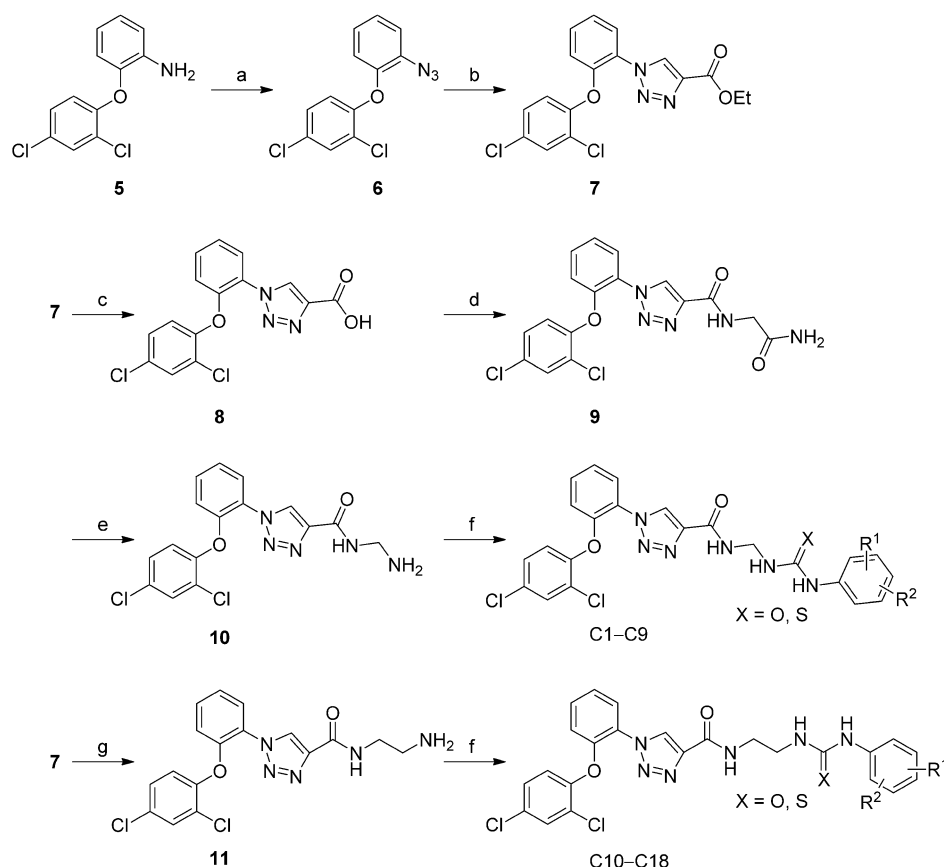
The binding mode of the lead compound to Mcl-1 predicted by molecular modeling suggested that the 2,4-dichlorophenyl group on the structure went into a cavity formed mainly by residues Met231, Met250, Val253, and Phe270 (Figure 2a). In order to explore the role of this moiety in binding, another similar set of thiophene-2-sulfonamide compounds, that is, YCW-E1–E21 (Table 4), were synthesized, in which a 3,4-dihydroxyphenyl or 3,4-dimethoxyphenyl moiety was introduced to replace the 2,4-dichlorophenyl moiety. In this case, the R^1 and R^2 groups are still the small-size electron-donating and electron-withdrawing substituent groups as in the other sets of compounds described above. The synthetic route for this set of compounds is outlined in Scheme 5 and is similar to that for the D compounds. The overall yields of the compounds with the 3,4-dihydroxyphenyl moiety turned out to be case dependent and ranged from 28–90%, whereas the overall yields of the compounds with the 3,4-dimethoxyphenyl moiety were generally over 90%. The purities of most of the compounds in this set are above 90% (with four exceptions).

Encouragingly, our binding assay results indicated that some E compounds have promising binding affinities to Mcl-1 and Bcl-2. The most potent compounds have inhibition constants of 0.3–0.4 μM for Mcl-1 (Table 4), values that are about 10-fold more potent than the lead compound. Some E compounds also exhibited apparent cytotoxicity ($IC_{50} < 10 \mu\text{M}$) on several tumor cell lines (Table 5). After a few failed attempts, we finally obtained some compounds, especially those E compounds with the 3,4-dihydroxyphenyl moiety, that have better potency for the target proteins and tumor cells than the lead compound. The binding of the E compounds to the target proteins and characterization of their apoptosis-inducing mechanism will be described and discussed in the following sections.

2. Binding of the thiophene-2-sulfonamide compounds to the Bcl-2 family proteins

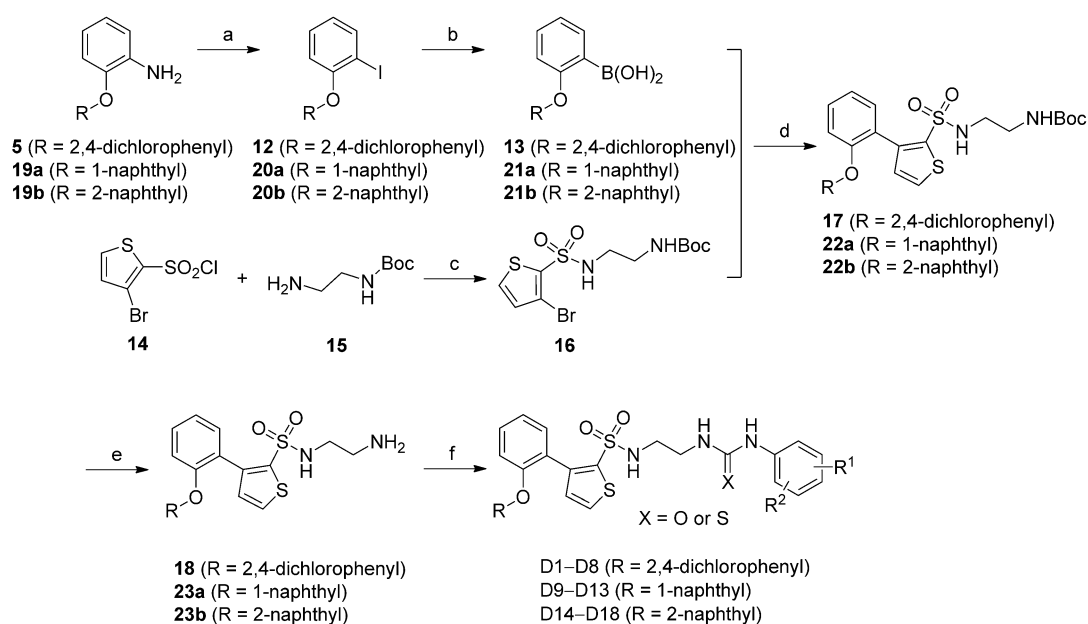
Compounds YCW-E1–E21 were tested in our FP-based assay to measure their binding affinities to the three target proteins, that is, Bcl- x_L , Bcl-2, and Mcl-1. Most of them have micromolar or sub-micromolar binding affinities to Bcl-2 and Mcl-1 (Table 4). The most potent compounds for Mcl-1 are YCW-E4, -E5, -E10, and -E11, which have inhibition constants between 0.3–0.5 μM . These four compounds are also the most potent ones on Bcl-2 with K_i values of around 1 μM . Another notable observation was that compounds YCW-E1–E11 have no or rather weak binding affinities to Bcl- x_L . The selectivity of our E compounds towards Mcl-1 and Bcl-2 is interesting among other known Bcl-2 inhibitors.

Two things regarding the structure–activity relationship of the E compounds need to be discussed in particular. Firstly, relative to the D compounds, the major difference in the YCW-E1–E11 compounds is the introduction of the 3,4-dihydroxyphenyl moiety. Given the fact that the D compounds do not have binding affinity to the three target proteins, this moiety apparently plays a critical role here. In fact, compounds YCW-E12–E21 were synthesized intentionally to replace the two hydroxy groups on this moiety with methoxy groups. The result-

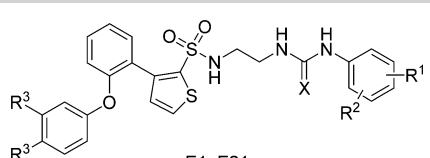


Scheme 3. Synthesis of compounds YCW-C1–C18. *Reagents and conditions:* a) 1. NaNO₂, H₂SO₄, 0 °C; 2. NaN₃, 0 °C → RT, 94%; b) CuI, CH₃CN, ethyl propiolate, RT, 76%; c) LiOH, MeOH, reflux, 99%; d) 4-methylmorpholine, EDCl, DMF, glycine hydrochloride, RT, 79%; e) CH₃CN, MeOH, PIFA, RT, 35%; f) aryl isothiocyanate, THF, RT; g) 1,2-ethanediamine, MeOH, reflux, 73%. EDCl: 3-(3-dimethylaminopropyl)-1-ethylcarbodiimide; PIFA: phenyliodine (III) bis(trifluoroacetate).

ing compounds indeed lost their binding affinities to Mcl-1 and Bcl-2 completely, which proved our speculation. Secondly, some of the active E compounds have a urea moiety instead of the thiourea moiety inherited from the lead compound. The binding affinities of these urea-containing compounds (YCW-E6–E11) are comparable to those of the thiourea-containing compounds (YCW-E1–E5). This trend is different from what was observed among the A/B compounds, among which only the thiourea-containing compounds have binding affinities to the target proteins. In addition, some A/B compounds have obvious binding affinities ($K_i=5\text{--}10\ \mu\text{M}$) to Bcl-x_L. In contrast, all of the E compounds have no or rather weak binding affinities to Bcl-x_L. Thus, the structure–activity relationship of the E compounds is notably different from that of the A/B compounds, despite the fact that these two sets of compounds share a certain level of structural similarity.



Scheme 4. Synthesis of compounds YCW-D1–D18. *Reagents and conditions:* a) 1. NaNO₂, H₂SO₄, 0 °C; 2. KI, 0 °C → RT; b) 1. nBuLi, THF, –78 °C; 2. B(OMe)₃; 3. HCl, RT; c) Et₃N, CH₂Cl₂, 0 °C → RT, 85%; d) Pd(OAc)₂, Sphos, K₃PO₄, THF, reflux, **17**: 50%, **22a**: 44%, **22b**: 61%; e) CF₃COOH, CH₂Cl₂, RT, **18**: 95%, **23a**: 95%, **23b**: 94%; f) aryl isothiocyanate, THF, RT. Sphos: dicyclohexylphosphino-2',6'-dimethoxybiphenyl; Boc: tert-butoxycarbonyl.

Table 4. Chemical structures and binding data for the E compounds.


Compd	X	E1–E21			Yield [%]	Bcl-x _L	K _i [μM] ^[a]	
		R ¹	R ²	R ³			Bcl-2	Mcl-1
YCW-E1	S	3-MeO	H	OH	39	N.A.	3.9 ± 0.8	17 ± 8.3
YCW-E2	S	3-NO ₂	H	OH	57	N.A.	1.7 ± 1.0	1.5 ± 0.2
YCW-E3	S	4-MeO	H	OH	45	weak	4.2 ± 0.9	2.0 ± 0.5
YCW-E4	S	4-NO ₂	H	OH	69	weak	1.2 ± 0.2	0.50 ± 0.07
YCW-E5	S	3-CF ₃	5-CF ₃	OH	85	weak	1.3 ± 0.2	0.39 ± 0.04
YCW-E6	O	3-MeO	H	OH	66	N.A.	3.2 ± 0.3	12.0 ± 4.4
YCW-E7	O	3-NO ₂	H	OH	82	N.A.	1.2 ± 0.2	2.2 ± 0.9
YCW-E8	O	4-MeO	H	OH	90	N.A.	3.1 ± 0.7	weak
YCW-E9	O	4-NO ₂	H	OH	35	N.A.	1.2 ± 0.3	0.98 ± 0.03
YCW-E10	O	3-CF ₃	5-CF ₃	OH	28	weak	1.2 ± 0.1	0.33 ± 0.03
YCW-E11	O	3-Cl	5-Cl	OH	69	weak	0.83 ± 0.05	0.33 ± 0.13
YCW-E12	S	H	H	OMe	99	N.A.	N.A.	N.A.
YCW-E13	S	3-NO ₂	H	OMe	97	N.A.	N.A.	N.A.
YCW-E14	S	4-MeO	H	OMe	79	N.A.	N.A.	N.A.
YCW-E15	S	4-NO ₂	H	OMe	97	N.A.	N.A.	N.A.
YCW-E16	S	3-CF ₃	5-CF ₃	OMe	95	N.A.	N.A.	N.A.
YCW-E17	O	3-NO ₂	H	OMe	97	N.A.	N.A.	N.A.
YCW-E18	O	4-MeO	H	OMe	92	N.A.	N.A.	N.A.
YCW-E19	O	4-NO ₂	H	OMe	94	N.A.	N.A.	N.A.
YCW-E20	O	3-Cl	5-Cl	OMe	91	N.A.	N.A.	N.A.
YCW-E21	O	3-CF ₃	5-CF ₃	OMe	87	N.A.	N.A.	N.A.

[a] The mean values and standard deviations of the K_i values were derived based on the outcomes of three parallel measurements. N.A.: No obvious sign of binding was observed; weak: dose-dependent FP signals were observed, but the change in the FP signals (up to 100 μM concentration) was not significant enough to determine the K_i value accurately.

In order to obtain some experimental proof for the binding mode of our active compounds, two-dimensional heteronuclear single quantum coherence (HSQC) spectroscopy was employed in our study. Three of the most promising compounds, that is, YCW-E5, -E10, and -E11, were selected to test their interactions with ¹⁵N-labeled Bcl-x_L in this experiment. ABT-737, a nanomolar binder to Bcl-x_L/Bcl-2, was used as the positive control here. Ideally, Mcl-1 or Bcl-2 should have been used in this experiment because our compounds exhibited tighter binding to Mcl-1 or Bcl-2 than Bcl-x_L. However, samples of ¹⁵N-labeled Mcl-1 or Bcl-2 were not available to us, so ¹⁵N-labeled Bcl-x_L was applied instead. Note that we concluded that YCW-E5, -E10, and -E11 have “weak” binding affinities to Bcl-x_L, based on the outcomes of our FP-based binding assay (Table 4). This means that a dose-dependent response in the FP signal was observed for the given compound, but the gross change in the FP signal was not significant enough, even at the highest concentration (100 μM) tested in our assay. Consequently, the inhibition constant of this compound could not be derived accurately. However, HSQC spectroscopy is a more sensitive technique for detecting weak bindings in the high-micromolar range. Thus, we expected that HSQC measurements for our compounds on Bcl-x_L could provide useful information.

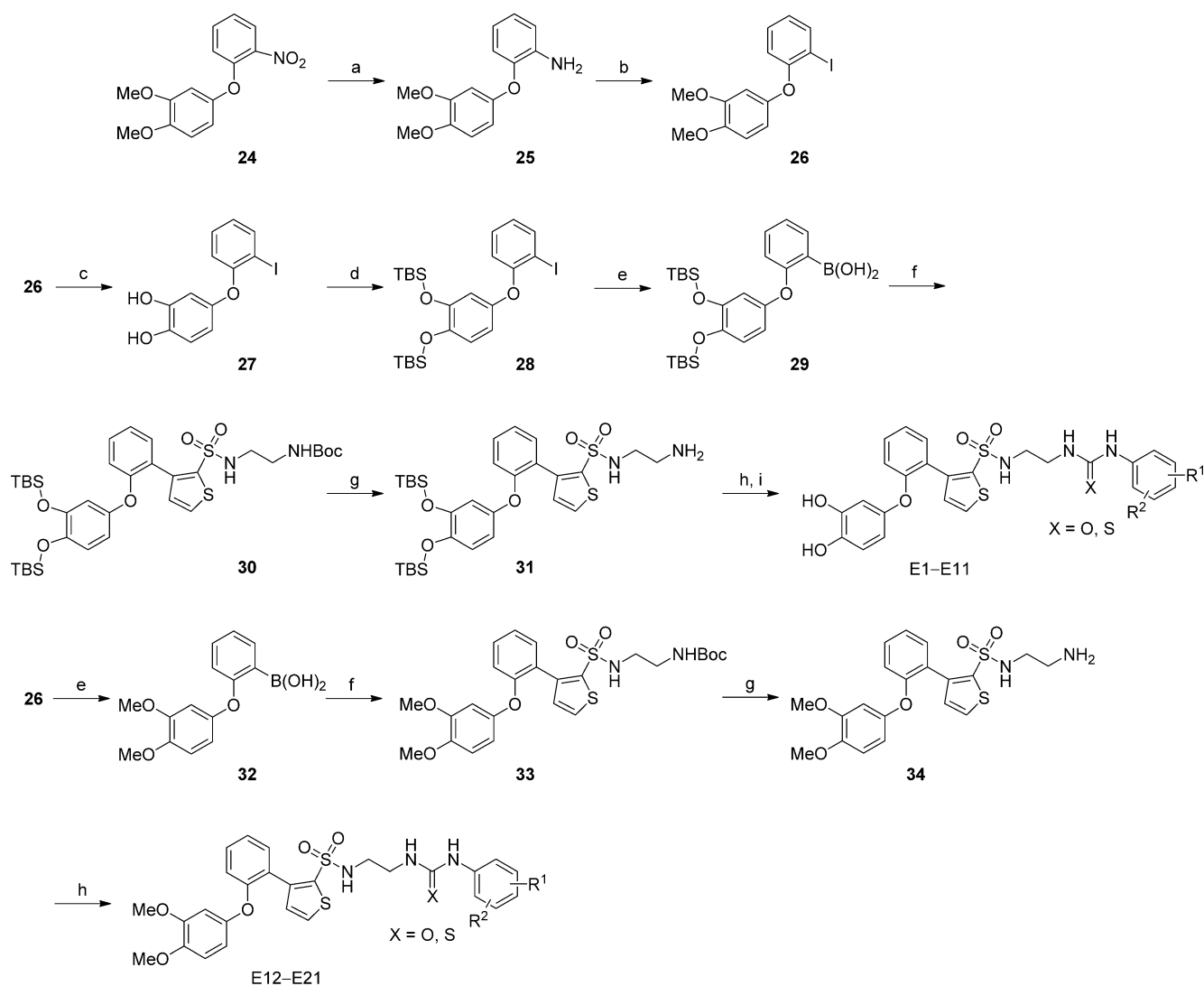
The obtained ¹⁵N-HSQC spectrum of Bcl-x_L with and without YCW-E5 is shown in Figure 3a as an example. The ¹⁵N-HSQC spectra of Bcl-x_L with YCW-E10, YCW-E11, and ABT-737 are given in the Supporting Information (part I). Many residues on Bcl-x_L exhibited apparent chemical shifts upon addition of YCW-E5 (Figure 3b). An overall similarity can be observed between the chemical shift patterns with YCW-E5 and ABT-737. To illustrate this point, the nine residues showing the largest chemical shifts (in Ω values) upon the addition of YCW-E5 are labeled on the complex structure formed by Bcl-x_L and ABT-737 in Figure 3c. One can see that these residues indeed surround the BH3-binding groove on Bcl-x_L, which suggests that YCW-E5 binds with Bcl-x_L with the same pattern as ABT-737. The results obtained on Bcl-x_L, of course, need to be transferred to Mcl-1 or Bcl-2 with care. However, because Mcl-1 and Bcl-2 do not really have a second major binding site on the molecular surface, it is reasonable to assume that YCW-E5, and the other active E compounds, also bind to Mcl-1 and Bcl-2 in the BH3-domain binding groove.

We then employed molecular modeling to derive the binding model of YCW-E5 to Mcl-1. This job was conducted through molecular docking, followed by molecular dynamics simulation to allow local conformation flexibility on the protein molecule. To make a comparison, the binding mode of the lead compound (BCL-VS-156) to Mcl-1 was also derived with the same methods. The final binding modes of the lead compound and YCW-E5 are shown in Figure 2a and b, respectively. Two subsites can be observed in

the BH3-binding groove on Mcl-1, which will be referred to as the

“L-site” and the “R-site” below according to their locations on the left or right in Figure 2. In a very recent work published by Tanaka et al.,^[34] these two sites are also referred to as the “western region” and the “eastern region”, respectively. The L-site is essentially hydrophobic and is formed mainly by Phe228, Met231, Met250, Val253, and Phe270. The R-site is more amphiphilic and is formed by hydrophobic residues, such as Val216, Val265, and Phe319, as well as the polar residues Asn260 and Arg263. In terms of shape, the L-site is deeper and more constrained, whereas the R-site is more open to the solvent. These two subsites are connected by a shallow channel, with His224 and Thr266 located on either side of it. Our predicted binding modes suggest that the 2-phenoxyphenyl moiety of both BCL-VS-156 and YCW-E5 is buried at the L-site, whereas the phenylurea (or phenylthiourea) moiety occupies the R-site. The remaining parts of the chemical structure, including the five-membered ring and the substituent group on it, go through the channel between the two subsites.

We hope to reach a qualitative explanation of the basic structure–activity relationship observed among our compounds with these predicted binding modes. The most important aspect in the binding modes of our compounds is how



Scheme 5. Synthesis of compounds YCW-E1–E21. *Reagents and conditions:* a) 10% Pd/C, 85% $\text{N}_2\text{H}_4\cdot\text{H}_2\text{O}$, EtOH, RT, 85%; b) 1. NaNO_2 , H_2SO_4 , 0°C ; 2. KI, 0°C \rightarrow RT, 87%; c) BBr_3 , CH_2Cl_2 , RT; d) TBSCl, imidazole, DMAP, CH_2Cl_2 , RT, 93% for 2 steps; e) 1. $n\text{BuLi}$, THF, -78°C ; 2. $\text{B}(\text{OMe})_3$; 3. HCl, RT, **28**: 93%, **32**: 55%; f) **16**, $\text{Pd}(\text{OAc})_2$, Sphos, K_3PO_4 , THF, reflux, **30**: 70%, **33**: 70%; g) CF_3COOH , CH_2Cl_2 , RT, **31**: 99%, **34**: 90%; h) aryl isothiocyanate, CH_2Cl_2 , RT; i) 40% HF, MeCN, RT. TBS: *tert*-butyldimethylsilyl; DMAP: 4-dimethylaminopyridine.

they fit into the L-site. Without exception, all known potent inhibitors of Bcl-2 family proteins are able to occupy the L-site. That is why we kept the 2-phenoxyphenyl moiety unchanged among the several sets of compounds synthesized by us. In particular, although the L-site is essentially hydrophobic, our model suggests that one of the two hydroxy groups on the terminal phenyl ring of YCW-E5 forms a hydrogen bond with the backbone amide group of Met250 (Figure 2b). This hydrogen bond becomes possible only after the L-site of Mcl-1 has undergone considerable conformational change. This seems to be a new feature of some small-molecule inhibitors of Bcl-2 family proteins that has been reported recently. For example, Lessene et al. reported that WEHI-539, a selective Bcl-X_L inhibitor with nanomolar potency, forms hydrogen bonds with the backbone amide groups of Ser106 and Leu108 at the L-site on Bcl-X_L (Protein Data Bank (PDB) entry 3ZLR).^[33] Our results showed that blocking these two hydroxy groups, as in com-

pounds YCW-E12–E21, led to a total loss of binding affinity to either Mcl-1 or Bcl-2, which indicates the importance of this possible hydrogen bond. This observation also suggests that the terminal 3,4-dihydroxyphenyl moiety on our E compounds fits into the L-site so tightly that even small extra methyl groups are not allowed.

The phenylurea moiety, which is at the other end of the chemical structure in our compounds, is predicted to occupy the R-site on Mcl-1. The binding data for the E compounds show that the introduction of a few different types of substituent groups onto the phenyl ring produces up to 50-fold difference in binding affinity to Mcl-1 and 5-fold difference in binding affinity to Bcl-2 (Table 4). The R-site is relatively wide and open, so the phenylurea moiety does not fit into it in a precise binding pose. In fact, it was observed to “swing” inside the R-site during the molecular dynamics simulation. It is not straightforward to interpret the effect on the binding affinity

Table 5. Cytotoxicity of the D and E compounds on six cell lines as measured in MTT assays.

Compd ^[a]	IC ₅₀ [μM] ^[b]					
	BEAS-2B	A549	H1299	HL-7702	7404	Hep3B
YCW-D9	> 100	> 100	> 100	> 100	> 100	> 100
YCW-D10	17	8	> 100	> 100	16	21
YCW-D11	> 100	> 100	> 100	> 100	> 100	> 100
YCW-D12	63	50	> 100	> 100	20	33
YCW-D13	4	5	15	33	2	10
YCW-D14	> 100	> 100	> 100	> 100	> 100	> 100
YCW-D15	0.3	12	19	26	8	21
YCW-D16	> 100	> 100	> 100	> 100	> 100	> 100
YCW-D17	11	23	36	64	11	15
YCW-D18	12	6	22	12	9	12
YCW-E1	2	> 100	> 100	> 100	> 100	> 100
YCW-E2	1	55	86	> 100	61	16
YCW-E3	7	> 100	> 100	> 100	> 100	> 100
YCW-E4	2	> 100	76	> 100	25	> 100
YCW-E5	4	4	7	8	6	14
YCW-E6	3	45	> 100	> 100	> 100	17
YCW-E7	2	> 100	> 100	> 100	> 100	> 100
YCW-E8	8	> 100	> 100	> 100	> 100	> 100
YCW-E9	3	> 100	> 100	> 100	> 100	> 100
YCW-E10	0.3	10	13	10	7	13
YCW-E11	0.9	21	46	29	10	> 100
YCW-E12	4	> 100	> 100	> 100	> 100	> 100
YCW-E13	0.7	18	> 100	> 100	30	> 100
YCW-E14	> 100	> 100	> 100	> 100	> 100	> 100
YCW-E15	0.6	20	> 100	41	9	> 100
YCW-E16	12	10	23	15	4	13
YCW-E17	0.6	26	43	> 100	> 100	66
YCW-E18	31	> 100	39	> 100	> 100	39
YCW-E19	2	13	21	13	17	88
YCW-E20	0.3	16	20	38	14	26
YCW-E21	13	12	32	22	8	13

[a] Compounds YCW-D1–D8 are not listed in this table because they were all inactive in this assay. [b] The concentration at 50% inhibition of cell growth (IC₅₀) values were derived from the outcomes of three parallel measurements.

of each substituent group on the phenyl ring. It seems that an increase in the dipole of the phenyl moiety with electron-withdrawing groups, such as CF₃, Cl, or NO₂, helps to achieve a tighter binding, especially to Mcl-1. We assume that some favorable dipole–dipole interactions may exist between this substituted phenyl moiety and some polar groups on the surrounding residues. However, this type of interaction may not be as specific and stable as hydrogen bonds.

Our predicted binding modes also suggest that the linker moiety, including the five-membered ring and the substituent group on it, also plays an important role. Firstly, this linker moiety has to take a bent conformation to allow the ligand molecule to fill up both the L-site and the R-site (Figure 2a and b). The tetrazole-2-acetamide moiety on the A/B compounds and the thiophene-2-sulfonamide on the E compounds are able to fulfill this requirement. In contrast, the linker moiety on the C compounds is basically a rigid planar fragment; thus, the C compounds cannot fill up the L-site and the R-site simultaneously with a low-energy binding pose. Secondly, the sulfonamide group on the E compounds may form hydrogen bonds with His224 and Thr266 on Mcl-1, which further

enhances the binding to Mcl-1. These two hydrogen bonds were fairly stable during the molecular dynamics simulations of this complex model (see the Supporting Information, part II). Note that His224 is conserved among Bcl-2 family proteins, but Thr266 is unique on Mcl-1. This may explain the moderate selectivity of the E compounds towards Mcl-1.

3. Characterization of the proapoptotic effects of thiophene-2-sulfonamide compounds

Three compounds, that is, YCW-E5, YCW-E10, and YCW-E11, were studied in four different types of assays to characterize their apoptosis-inducing effects on HL-60 cells. The HL-60 cell line was chosen because it is known to overexpress Bcl-2 family proteins and is often used for testing Bcl-2 inhibitors.^[7,8] These three compounds were chosen because they were the most potent ones in the binding assay and they also exhibited obvious cytotoxicity on tumor cells. ABT-737 was used as the positive reference in all four assays.

In the first assay, flow cytometry was employed to detect whether the compounds under test could induce apoptosis in HL-60 cells. In this assay, viable cells were negative for both propidium iodide (PI) and annexin V. The cells undergoing early apoptosis were positive for annexin V and negative for PI, whereas the cells undergoing late apoptosis and nonviable cells, which could undergo apoptosis or necrosis, displayed both high annexin V and PI labeling. Cell debris was positive for PI and negative for annexin V. The fluorescence of annexin V and PI measured in our assays for ABT-737 and three other compounds are given in the Supporting Information (part III). A graphical summary of the results is given in Figure 4. One can see that upon treatment with the three E compounds at a concentration of around 10 μM after 24 h, up to 60% cells were observed to undergo early apoptosis. In addition, the apoptosis-inducing effect of all three compounds is clearly dose-dependent. In this assay, YCW-E5 and YCW-E10 are marginally more potent than YCW-E11. However, they are all at least 10-fold less potent than ABT-737. This level of difference is understandable because ABT-737 is a highly potent inhibitor of Bcl-x_L/Bcl-2 ($K_i < 1 \text{ nM}$). Our compounds still need optimization to improve the potency.

The second assay detected poly-ADP-ribose polymerase protein (PARP) cleavage and caspase-9 activation, both of which are hallmarks of apoptosis through the mitochondrial pathway, upon treatment of HL-60 cells with the given compounds. PARP is a major substrate for activated caspases. Our western blot results showed that the full-length PARP (116 kDa) was degraded and the cleaved PARP (89 kDa) increased, relative to the results with the control group, after treatment with ABT-737 or the other three given compounds (Figure 5). It was also observed that the precursor procaspase-9 (47 kDa) was degraded and the level of cleaved caspase-9 (35 kDa and 37 kDa) increased after treatment with the compounds (Figure 5).

The outcomes of the second assay suggested that our compounds are able to induce apoptosis through the mitochondrial pathway, like ABT-737 does. Thus, the next assay investigated the effects of the given compounds on the mitochondrial

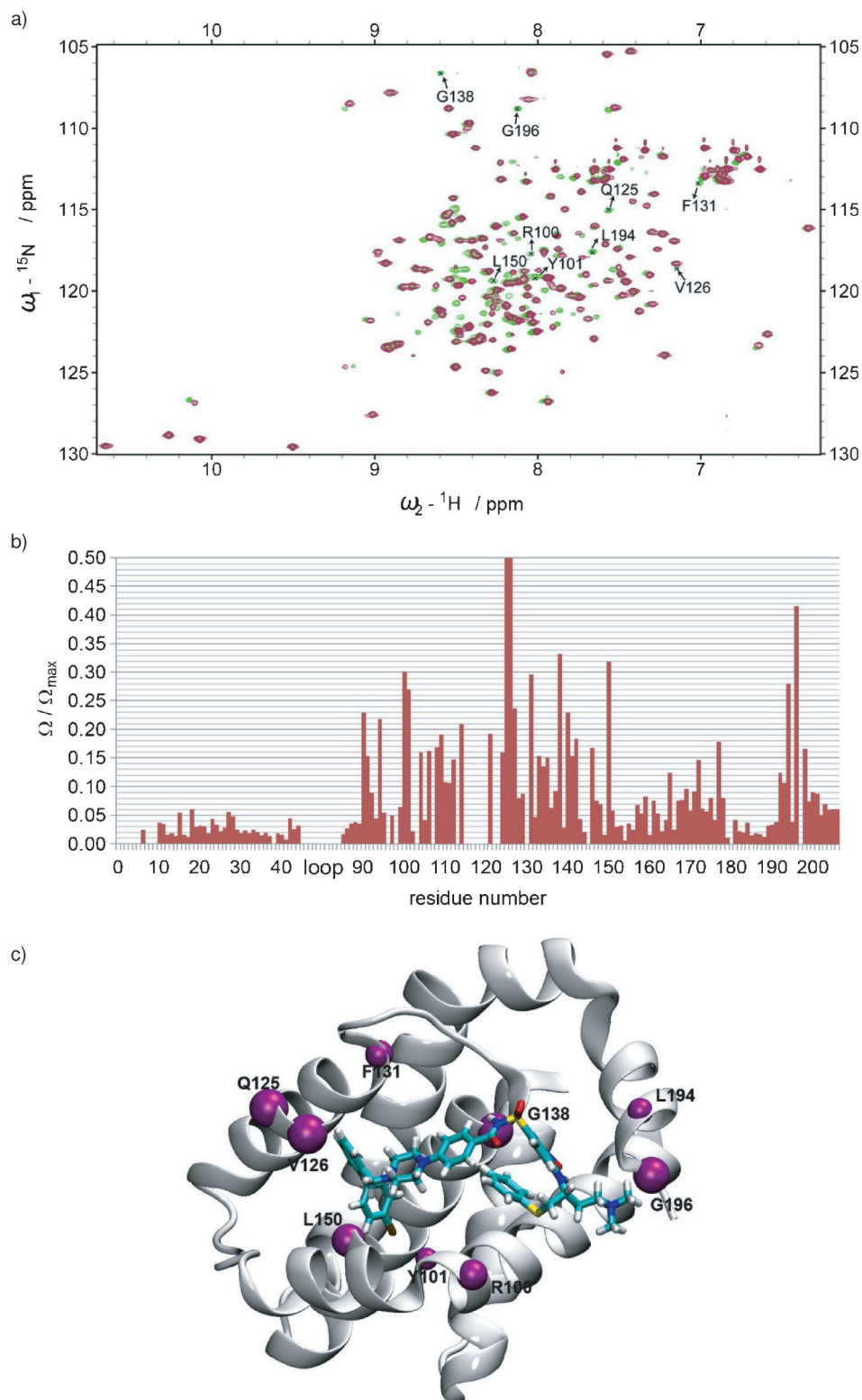


Figure 3. a) Superimposed ^{15}N -HSQC spectra of free Bcl- x_L (in green) and Bcl- x_L in complex with compound YCW-E5 (in red). The nine residues with the largest chemical shifts (in Ω values) are labeled explicitly. b) Normalized Ω values of all residues on Bcl- x_L upon binding with YCW-E5. c) The known complex structure formed by Bcl- x_L with ABT-737 (PDB entry 2YXJ), in which ABT-737 is shown as a stick model and the backbone of Bcl- x_L is shown as gray ribbons. Locations of the nine residues with the largest chemical shifts upon binding with YCW-E5 are indicated by purple spheres on this structure, which indicates that this compound binds at the same site on Bcl- x_L as ABT-737.

membrane potential ($\Delta\psi_m$). The $\Delta\psi_m$ value was monitored by using the fluorescent dye Rh123. It is a cell-permeable cationic dye, which preferentially partitions into the mitochondria as a result of their highly negative $\Delta\psi_m$ value. Mitochondrial membrane depolarization results in the loss of Rh123 from the mitochondria, and a decrease in intracellular fluorescence. The Rh123 fluorescence intensities measured on HL-60 cells after 24 h of treatment with the given compounds are given in the Supporting Information (part III). A graphical summary of the results is given in Figure 6. All of the three E compounds exhibited obvious dose-dependent effects on the $\Delta\psi_m$ value, like ABT-737 does.

The last assay detected the release of cytochrome c, which is another hallmark of apoptosis through the mitochondria pathway. In this assay, mitochondria isolated from untreated HL-60 cells were treated with the given compounds. Cytochrome c in the mitochondrial supernatants and pellets was then detected by western blot experiments. As compared with the control group, the amount of cytochrome c in the mitochondrial pellets was reduced, whereas the amount of cytochrome c in the mitochondrial supernatants was increased upon treatment with any of the three E compounds (Figure 7). Again, ABT-737 exhibited a stronger effect than our E compounds, which is understandable when the high potency of this compound is considered.

Conclusions

In this study, we aimed at optimizing a lead compound, which was originally discovered through structure-based virtual screening, as an inhibitor of anti-apoptotic Bcl-2 family proteins.

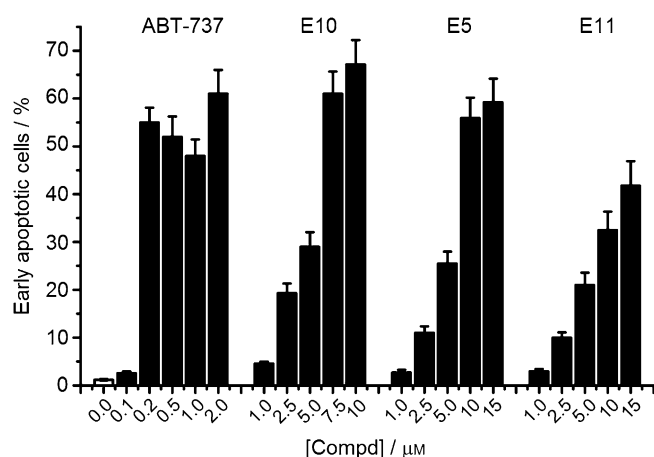


Figure 4. Early apoptosis in HL-60 cells induced after 24 h of treatment of the given compounds. Cells with annexin V and PI double staining were examined by flow cytometry to detect the occurrence of early apoptosis.

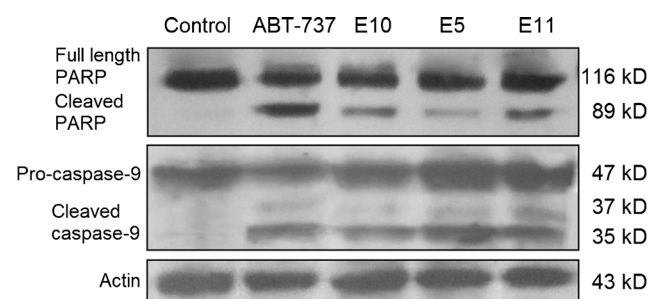


Figure 5. PARP cleavage and caspase-9 activation in HL-60 cells detected in a western blot experiment. Cells were treated with ABT-737 (1 μM), YCW-E10 (7.5 μM), YCW-E5 (10 μM), and YCW-E11 (15 μM) at 37 °C for 24 h. Actin was used as the protein loading control.

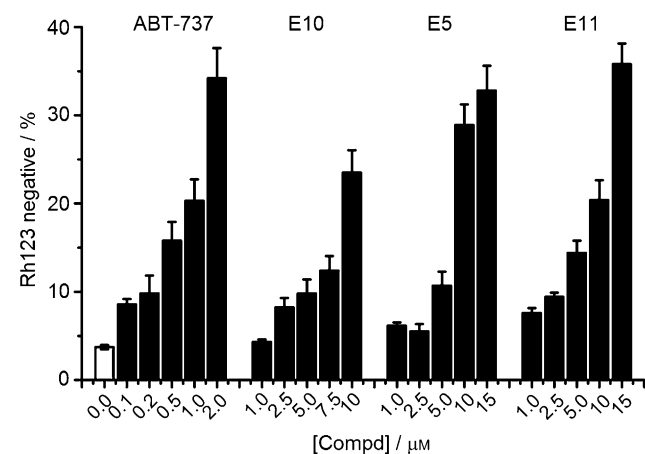


Figure 6. Percentage of Rh123-negative HL-60 cells after 24 h of treatment of the given compounds. All of the compounds under test exhibited obvious, dose-dependent effects on the mitochondrial membrane potential.

This compound contains a phenyltetrazole moiety and a hydrazinecarbothioamide moiety and, therefore, represents a structural scaffold not observed among known Bcl-2 inhibitors. We first synthesized a set of 25 derivative compounds with the phenyltetrazole moiety, that is, the A/B compounds. This set of

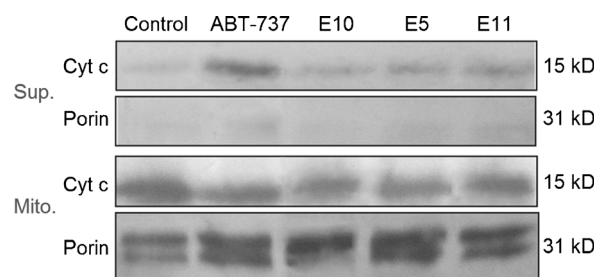


Figure 7. Cytochrome c in mitochondrial supernatants and pellets detected in a western blot experiment. Mitochondria isolated from untreated HL-60 cells were incubated with ABT-737 (2 μM) or the three tested compounds (5 μM) at 37 °C for 30 min. The mitochondria pellets (Mito.) and supernatants (Sup.) were then obtained by centrifugation. Porin was used as the mitochondria loading control.

compounds do have micromolar binding affinities to the three target proteins. However, they are not effective apoptosis inducers on living tumor cells due to poor cell permeability. Next, we synthesized a second set of 18 compounds by replacing the phenyltetrazole moiety with a phenyltriazole moiety, that is, the C compounds. This set of compounds can be synthesized neatly, but unfortunately, they do not have the desired biological activities. We then synthesized the third set of 39 compounds with a 3-phenylthiophene-2-sulfonamide moiety, that is, the D/E compounds. Encouragingly, some compounds among them exhibited both promising binding affinities to the target proteins and obvious cytotoxicity on tumor cells. The most potent compounds, that is, those E compounds with a terminal 3,4-dihydroxyphenyl moiety, have sub-micromolar binding affinities to Mcl-1 ($K_i = 0.3\text{--}0.4\ \mu\text{M}$) or Bcl-2 ($K_i \approx 1\ \mu\text{M}$). As compared with the lead compound, these compounds are about 10-fold more potent and also easier to synthesize. Their selectivity towards Mcl-1 and Bcl-2 is also interesting.

Three selected compounds, that is, YCW-E5, YCW-E10, and YCW-E11, were studied in several apoptosis assays conducted on HL-60 cells. Our results demonstrated that they are able to induce cell apoptosis through the mitochondrial pathway. It remains to be confirmed that these compounds induce apoptosis through Bcl-2/Mcl-1 inhibition in living cells by appropriate assays. But, in every experiment that we have conducted, these compounds caused similar effects to ABT-737, which suggests that these compounds may target the antiapoptotic Bcl-2 family proteins in living cells. We propose that the compounds with the 3-phenylthiophene-2-sulfonamide core moiety are worth further optimization as effective apoptosis inducers.

Experimental Section

Organic synthesis

General: All reagents and starting materials used in the syntheses were purchased from Lancaster, Acros, and Shanghai Chemical Reagent Corp. and were used without further purification unless specified.

All NMR spectra were recorded at RT on a Bruker AV-400 400 MHz spectrometer. They were calibrated by using residual CHCl_3 ($\delta_{\text{H}} = 7.26$ ppm) and CDCl_3 ($\delta_{\text{C}} = 77.16$ ppm) or CH_3OH ($\delta_{\text{H}} = 3.31$ ppm) and CD_3OD ($\delta_{\text{C}} = 49.00$ ppm) as internal references. The following abbreviations are used to designate multiplicities: s: singlet; d: doublet; t: triplet; q: quartet; m: multiplet; quint: quintet; br: broad. High-resolution mass spectrometry (HRMS) was performed on a Bruker APEXIII 7.0 Tesla ESI-FT mass spectrometer at a 4000 V emitter voltage. The purity of the final compounds was determined by the analytical HPLC method. An Agilent 1100 series HPLC with an Agilent Zorbax Eclipse SB-C18 (4.6 mm, 5 μm particle sizes) reversed-phase column was used to perform analytical HPLC analyses. The elution buffer was a gradient of $\text{H}_2\text{O}/\text{CH}_3\text{OH}$.

Synthetic protocols and characterization data for intermediates **2**–**34** are given in the Supporting Information, along with spectral data for all of the target compounds (YCW-A1–A13, B1–B12, C1–C18, D1–D18, and E1–E21). For the synthesis of compounds *not* described in the Supporting Information, please provide complete protocols and missing details (equivalents/reaction times/reaction temperatures/yields etc.) to allow other to repeat your work.

General procedure for the synthesis of YCW-A1–A13 and YCW-B1–B12 (Scheme 2)

Compound **2** was obtained through the reaction of **1** with NaN_3 in the presence of $\text{Et}_3\text{N}\cdot\text{HCl}$ as a catalyst with heating at reflux in DMF for 12 h. Compound **2** was further treated with methyl bromoacetate in the presence of NaH as a base with heating at reflux in THF for 5 h to give **3a** and **3b**. The reaction of **3a** or **3b** with $\text{NH}_2\text{NH}_2\cdot\text{H}_2\text{O}$ with heating at reflux in THF for 12 h gave **4a** or **4b**, respectively. Detailed procedures for each step are described in the Supporting Information.

A solution of **4a** in THF (3 mL) was treated with the appropriate aryl isothiocyanate or isocyanate (1.2 equiv). The solution was heated at reflux until the starting material disappeared. Then, the reaction was cooled, concentrated and purified by chromatography (EtOAc/petroleum ether 3:1) to obtain compounds YCW-A1–A13 as solids with yields ranging from 59–89% (Table 1). The reaction of **4b** with the appropriate aryl isothiocyanate or isocyanate under analogous conditions gave YCW-B1–B12 with yields ranging from 84–91% (Table 1).

General procedure for the synthesis of compounds YCW-C1–C18 (Scheme 3)

Aniline **5** was diazotized by NaNO_2 and aq H_2SO_4 at 0°C and then treated with NaN_3 from 0°C to RT to give azide **6** in high yields. Compound **7** was obtained by the reaction of **6** with ethyl propionate in the presence of CuI as the catalyst in CH_3CN at RT. Saponification of **7** by LiOH in MeOH gave acid **8**. EDCl-mediated condensation of **8** with glycylamide hydrochloride in DMF at RT gave amide **9**, which was then treated with PIFA to obtain **10** through the Hofmann rearrangement. The reaction of **7** with 1,2-ethanediamine and with heating at reflux in MeOH gave **11**. Detailed procedures for each step are described in the Supporting Information.

A solution of **10** (50 mg) in THF (3 mL) was treated with the appropriate aryl isothiocyanate (1.2 equiv). The solution was stirred at RT until the starting material disappeared. Then, the solvent was removed under reduced pressure. The residue was purified by chromatography (EtOAc/petroleum ether 1:1) to obtain compounds YCW-C1–C9 with yields ranging from 86–93% (Table 2). The reaction of **11** with the appropriate aryl isothiocyanate under analogous conditions gave YCW-C10–C18 with yields ranging from 76–92% (Table 2).

General procedure for the synthesis of compounds YCW-D1–D18 (Scheme 4)

Aniline **5** was diazotized by NaNO_2 and aq H_2SO_4 at 0°C and then treated with KI from 0°C to RT to give **12**. Boronic acid **13** was produced from **12** through lithium–halogen exchange at -78°C in THF, followed by borate trapping and then hydrolysis in 1.0 M HCl solution. The reaction of **14** with **15** in CH_2Cl_2 from 0°C to RT gave **16**. Suzuki cross-coupling between **13** and **16** catalyzed by $\text{Pd}(\text{OAc})_2$ and Sphos with heating at reflux in THF gave **17**. Removal of the Boc group on **17** by CF_3COOH in CH_2Cl_2 at RT gave **18**. Boronic acids **21** were synthesized from aniline **19** following the same procedure as described for **13**. Suzuki cross-coupling between **21** and **16** and subsequent steps to access **23** were performed as for **18**. Detailed procedures for each step are described in the Supporting Information.

A solution of **18** (60 mg) in THF (3 mL) was treated with the appropriate aryl isothiocyanate (1.1 equiv). The solution was stirred at RT until the starting material disappeared. Then, the solvent was removed under reduced pressure. The residue was purified by chromatography (EtOAc/petroleum ether 1:1) to obtain compounds YCW-D1–D8 as solids with yields ranging from 95–99% (Table 3). The reaction of **23** with the appropriate aryl isothiocyanate under analogous conditions gave YCW-D9–D18 with yields ranging from 89–99% (Table 3).

General procedure for the synthesis of compounds YCW-E1–E21 (Scheme 5)

Compound **24** was reduced by 85% $\text{N}_2\text{H}_4\cdot\text{H}_2\text{O}$ in the presence of Pd/C in EtOH at RT to give aniline **25**. Compound **25** was diazotized by NaNO_2 and aq H_2SO_4 at 0°C and then treated with KI from 0°C to RT to give **26**. The methyl groups were removed by BBr_3 in CH_2Cl_2 at RT, and then the diol group was protected with TBS to give **28**. Boronic acid **29** was produced from **28** through lithium–halogen exchange at -78°C in THF followed by borate trapping. Suzuki cross-coupling between **29** and **16** catalyzed by $\text{Pd}(\text{OAc})_2$ and Sphos was conducted with heating at reflux in THF. The removal of the Boc group by CF_3COOH in CH_2Cl_2 at RT gave **31**. Boronic acid **32** was produced from **26** in an analogous way to **29** described above. Suzuki cross-coupling between **32** and **16** and then removal of the Boc group gave **34**. Detailed procedures for each step are described in the Supporting Information.

A solution of **31** (70 mg) in CH_2Cl_2 (3 mL) was treated with the appropriate aryl isothiocyanate (1.2 equiv). The solution was stirred at RT until the starting material disappeared. Then, the solvent was removed under reduced pressure to obtain the protected intermediate. To remove the TBS groups, the intermediate was dissolved in a solution of CH_3CN (2 mL) and 40% HF (0.2 mL). The solution was stirred at RT until the intermediate disappeared. The solution was diluted with EtOAc and washed with distilled H_2O and then saturated aq NaCl. The organic layer was collected and dried by anhyd Na_2SO_4 . The residue was filtered and condensed and purified by chromatography (EtOAc/petroleum ether 1:1) to obtain compounds YCW-E1–E11 as solids with yields ranging from 28–90% (Table 4). The reaction of **34** with the appropriate aryl isothiocyanate under analogous conditions described for the reaction of **31** (deprotection not required) gave YCW-E12–E21 with yields ranging from 79–99% (Table 4).

In vitro binding assays

An FP-based assay was employed in this study to measure the binding affinities of small-molecule compounds to three antiapop-

totic Bcl-2 family proteins, including Mcl-1, Bcl-x_L, and Bcl-2. The 5-FAM-Bid-BH3 peptide, that is, a 26-residue peptide (QEDIIR-NIARHLAQVGDSDMRISPPG) with a 5-carboxyfluorescein (5-FAM) label on its N terminus, was used as the fluorescence tracer in this assay. In each measurement, the target protein was incubated with the Bid-BH3 peptide first, and then competitive binding of the given compound was monitored by FP signal changes upon addition of the compound in multiple doses. Methods for preparing the protein samples and detailed experimental settings in the FP measurement can be found in the Supporting Information (part V).

In this study, each compound was initially tested at three concentrations of 1, 10, and 50 μM against all three target proteins (Mcl-1, Bcl-x_L, and Bcl-2). At each concentration, the average FP values (in mP units) of three parallel measurements were used to compute the inhibition ratio by using Equation (1).

$$\text{Inhibition [\%]} = \frac{mP_{\text{max}} - mP_{\text{test}}}{mP_{\text{max}} - mP_{\text{NC}}} \quad (1)$$

Here, mP_{max} refers to the FP signal detected when the protein was incubated with the Bid-BH3 peptide, mP_{NC} refers to the FP signal detected from the negative control, that is, the Bid-BH3 peptide alone, and mP_{test} refers to the FP signal detected when the compound under test was added at a certain concentration. If the compound under test showed obvious dose-dependent competitive binding to the target protein and it achieved an inhibition ratio over 50% at 50 μM, it was then further tested at 7 different concentrations of 1, 10, and 100 nM and 1, 10, 50, and 100 μM, to obtain a complete dose-dependent binding curve. The binding curve was derived through nonlinear fitting by using the GraphPad Prism software (version 5; <http://www.graphpad.com/>). The concentration of the given compound at which 50% of the bound peptide was displaced (IC₅₀) was derived from the binding curve. The competitive inhibition constant of the compound under test was calculated with a mathematical equation developed by Wang and co-workers,^[44] with the assumption that it formed a binary complex with the target protein.

¹⁵N-Heteronuclear single quantum coherence spectroscopy

The Bcl-x_L protein used in this experiment was a special truncated construction of the full-length protein, with deletion of residues 45–84 on a long loop region and residues 210–233 at the C terminus, which has been reported repeatedly in the literature for solving Bcl-x_L structures. This construction was proven to retain the biological function of the wild type.^[45] An 8×His tag was added to the N terminus. This protein was cloned into the pSJ2 vector (a modified vector based on pET28a) at the EcoRI and XhoI sites, by using the following oligonucleotides: 5'-TCTCGAATTCATGTCTCAGAGCAACCGGA-3' and 5'-GGTCCTCGAGTCAGCGTTCCTGGCCCTTCG-3'. It was expressed in *Escherichia coli* BL21(DE3) cells. Cells were grown at 37 °C in M9 medium containing ¹⁵N-ammonium chloride and 1 mM ampicillin to an optical density at 600 nm (OD₆₀₀) of 0.6. Protein expression was induced by addition of 0.4 mM isopropyl-β-D-thiogalactopyranoside (IPTG) at 20 °C for 16 h. Cells were lysed in 25 mM tris(hydroxymethyl)aminomethane (Tris)-HCl buffer at pH 7.0 containing 100 mM NaCl and 0.1 mg mL⁻¹ phenylmethanesulfonyl fluoride (PMSF). ¹⁵N-labeled His-TEV-Bcl-x_L protein was purified from the soluble fraction by using Ni-NTA resin (Qiagen). The ¹⁵N-labeled His-TEV-Bcl-x_L protein was further cleaved by TEV protease (0.5 mg mL⁻¹, 4 °C, 12 h) to obtain ¹⁵N-labeled Bcl-x_L protein. The ¹⁵N-labeled Bcl-x_L protein was

then purified on Superdex75 (GE Healthcare) in phosphate-buffered saline (PBS) solution.

¹⁵N-Heteronuclear single quantum correlation (HSQC) NMR spectra were recorded on a Bruker DMX 600 MHz NMR spectrometer at 25 °C with samples containing 200–500 μM ¹⁵N-labeled protein. The ratio of each tested compound and the Bcl-x_L protein in the sample was 1:1. The resulting NMR spectra were processed and analyzed by using the nmrPipe and nmrDraw software (<http://spin.niddk.nih.gov/NMRPipe/>). The HSQC spectrum of free Bcl-x_L, which is publicly available from the Biological Magnetic Resonance Data Bank (<http://www.bmrb.wisc.edu/>; access number: 18250), was adopted as the reference for the assignment of chemical shifts. In order to quantify the chemical shift of each residue on the two-dimensional HSQC spectra, the Ω value was computed by using Equation (2).

$$\Omega = \sqrt{(0.2 \cdot \Delta\delta^{15\text{N}})^2 + (\Delta\delta^1\text{H})^2} \quad (2)$$

In this study, three compounds, that is, YCW-E5, -E10, and -E11, were selected to be tested by using the protocols described above. ABT-737, a well-known Bcl-2 inhibitor that binds to the BH3 binding groove on Bcl-x_L, was also tested as a positive reference.

Molecular modeling

The binding modes of the lead compound BCL-VS-156 and of YCW-E5 to Mcl-1 were predicted by molecular modeling. As the first step, molecular docking was employed to derive a rough binding mode for each given molecule. The complex structure formed between human Mcl-1 and the mNoxaB-BH3 peptide (PDB entry 2NLA)^[46] was used for this task. The molecular structures of BCL-VS-156 and YCW-E5 were sketched with the SYBYL software (version 8.1; <http://www.certara.com/>) and then optimized with the MMFF94 force field. Automatic docking of each molecule to Mcl-1 was performed by using the GOLD software (version 5.1, Cambridge Crystallographic Data Centre, <http://www.ccdc.cam.ac.uk/>). The binding site on Mcl-1 for performing docking was defined as all amino acid residues within 10 Å from Thr266, a residue roughly at the center of this binding site. The GOLD software employs a genetic algorithm (GA) to control the docking process. In our study, the whole population was placed on 5 separate islands with 100 individuals on each island. The total number of GA operations to be performed was set to 100 000. Probabilities for crossover, mutation, and migration operations were set to 95, 95, and 10, respectively. The ChemPLP scoring function was adopted to compute the binding scores. A total of 30 final binding poses were generated for the input molecule. These binding poses were clustered with a root mean square deviation (RMSD) cutoff of 1.5 Å by using the "rms_analysis" tool included in the GOLD package. Among the binding poses with the highest binding scores in each cluster, one was selected as the most reasonable one after visual examination.

The selected binding pose of the given molecule was then refined through molecular dynamics (MD) simulation by using the AMBER program (version 9, University of California, San Francisco; <http://www.ambermd.org/>). The MD simulation was performed in an explicit water box for 10 ns. To set up the job, the force-field parameters applied to the small-molecule ligand were prepared by applying the Antechamber module in the AMBER program. Atomic partial charges on the small-molecule ligand were derived with the RESP method, based on the HF/6-31G* computation results given by the Gaussian software (version 09, released by Gaussian Inc.; <http://www.gaussian.com/>). Atoms on the Mcl-1 protein were as-

signed the PARM99 template charges implemented in the AMBER program. All ionizable residues were set at their default protonation states under a neutral pH value. The complex structure was soaked in a box of TIP3P water molecules with a margin of 10 Å along each dimension. An appropriate number of counter ions were added to neutralize the whole system. After these preparations, the complex structure was first relaxed by 100 cycles of steepest descent minimization, followed by 4900 cycles of conjugated gradient minimization. In this process, the protein and the ligand were constrained with a constant of $10.0 \text{ kcal mol}^{-1} \text{ \AA}^2$. After that, the whole system was further relaxed by 5000 cycles of minimization without constraints. The whole system was then heated up gradually from 0 to 300 K in 100 ps, followed by 10 ns MD simulation at a constant temperature of 300 K and a constant pressure of 1 atm. During simulation, electrostatic interactions were calculated with the PME algorithm, and the distance cutoff of nonbonded interactions was set as 12 Å. The SHAKE algorithm was applied to fix the lengths of all chemical bonds connecting hydrogen atoms. On the final MD trajectory, a total of 10 000 snapshots were retrieved at 1 ps interval. These snapshots were grouped into clusters based on mass-weighted RMSD values with a cutoff value of 1.5 Å. The snapshot closest to the cluster center in the largest cluster was selected as the representative model of the given complex. The final models of BCL-VS-156 and YCW-E5 binding to Mcl-1 are shown in Figure 2a and b. More details of these two models are given in the Supporting Information (part II).

Cytotoxicity assay

The cytotoxic activities of our compounds were tested by the standard MTT assay on six cell lines. This assay served as a basic measure in our study for characterizing the cell permeability of our compounds. These six cell lines included the human liver tumor cells 7404 and Hep3B, with normal liver HL-7702 cells as a control, and the human lung tumor cells A549 and H1299, with human bronchial epithelial BEAS-2B cells as a control. All cell lines were originally obtained from the American Type Culture Collection (ATCC, Manassas, VA) and were cultured in Dulbecco's modified Eagle's medium (DMEM; H1299, Hep3B), RPMI-1640 medium (BECM; HL-7702, and 7404), or Beltsville embryo culture medium (BECM; BEAS-2B) with 10% fetal bovine serum (FBS) and supplemented with 1% penicillin/streptomycin (P/S). Cell Counting Kit-8 (CK-04) was bought from Dojindo (Kumamoto, Japan) for the cytotoxicity assay. All of the tested compounds were dissolved to three concentrations of 0.50, 5.0, and 50 μM , respectively, in which the DMSO concentration in each final solution was lower than 0.04%. Cytotoxicity was determined by using Cell Counting Kit-8 (CCK-8, Dojindo, Japan). In each test, 4000 cells were seeded in each well on 96-well plates, which were then treated with the given compound at the three final concentrations for 48 h. After treatment, the CCK-8 solution (10 μL) was added to each well. Plates were incubated for an additional 2–4 h at 37 °C. The supernatant was carefully removed, and DMSO (100 μL) was added to dissolve the formazan crystals. The absorbance at 450 nm was then recorded by using a SpectraMax-190 microplate reader (Molecular Devices, USA) to calculate the inhibition rates. If necessary, the concentration at 50% inhibition (IC_{50}) of each tested compound was derived through nonlinear fitting of the average inhibition rates read from three independent wells.

Apoptosis mechanism studies

Cell culture and treatment of compounds: Human HL-60 promyelocytic leukemia cells (ATCC, Manassas, VA) were cultured in RPMI-1640 medium (Hyclone) supplemented with 10% (v/v) FBS (Hyclone), 100 g mL^{-1} streptomycin (Gibco), and 100 IU mL^{-1} penicillin (Gibco). Cells were incubated under a 5% CO_2 humidified atmosphere at 37 °C. Cells were seeded into a 75 cm^2 Corning cell culture flask (for mitochondria isolation) or 6- or 12-well cell culture plates (for drug stimulation) and maintained by addition of new medium every day. Cells were plated at a density of $5 \times 10^5 \text{ mL}^{-1}$ 24 h prior to compound treatment. Before mitochondria isolation or drug induction of normal cells, cell viability was confirmed to be >95% by using the trypan blue exclusion assay. ABT-737 and other tested compounds were dissolved in DMSO to a final concentration lower than 0.1%. The control cells were treated with the same volume of the vehicle. The medium was cultured in the presence or absence of multiple concentrations of ABT-737 (0, 0.10, 0.20, 0.50, 1.0, and 2.0 μM) or tested compounds (YCW-E10: 0, 1.0, 2.5, 5.0, 7.5, and 10 μM ; YCW-E5 and E11: 0, 1.0, 2.5, 5.0, 10, and 15 μM) for 24 h, respectively. Three parallel experiments were conducted for each compound under the same conditions.

Flow cytometry analysis: The number of apoptotic cells induced by the tested compounds was measured by flow cytometry with an Alexa Fluor 488 Annexin V/Dead Cell Apoptosis Kit. The annexin V-PI assay evaluates phospholipids turning over from the inner to the outer lipid layer of the plasma membrane, an event typically associated with apoptosis. After being treated with ABT-737 or target compounds at different concentrations for 24 h, HL-60 cells were harvested and washed with cold PBS. Cell pellets were suspended in $1 \times$ binding buffer at a concentration of $1 \times 10^6 \text{ cells mL}^{-1}$. Annexin V-Alexa Fluor 488 (5 μL) and PI (1 μL ; the final concentration of PI was 1 $\mu\text{g mL}^{-1}$) were added to cell suspension (100 μL) and vortexed gently. The stained samples were incubated for 15 min at RT in the dark. An additional portion (400 μL) $1 \times$ binding buffer was added to each tube. Samples were analyzed by a flow cytometer (FACSaria, BD Biosciences) equipped with BD FACSDiva software (BD Biosciences) within 1 h. A total of 10 000 events were acquired by using the green channel FL1 for Annexin V-Alexa Fluor 488 and the red channel FL3 for PI. Data presented in this work were representative of those obtained from at least three independent experiments done in triplicate.

Western blot detection of caspase-9 activation: HL-60 cells were lysed in lysis buffer (1% Triton X-100, 50 mM Tris (pH 7.4), and 150 mM NaCl, containing protease inhibitors (Complete, Roche)) maintained on ice and vortexed gently every 10 min. The sample was centrifuged for 15 min at 12 000 g and 4 °C to get rid of cell debris. The protein concentration was assayed by using bicinchoninic acid (Pierce). The cytosolic protein (40 μg) was then subjected to electrophoresis on 10% sodium dodecylsulfate (SDS) polyacrylamide gels, by using a Bio-Rad mini-gel apparatus, and blotted to polyvinylidene difluoride (PVDF) membranes (Millipore, MA, USA) through electrotransfer. Membranes were blocked for 1 h with 5% nonfat dry milk in Tris-buffered saline containing 0.1% Tween-20 (TBST) and then incubated with antibodies (mouse monoclonal anti-caspase-9 antibodies at a 1:1000 dilution, rabbit monoclonal anti-PARP antibodies at a 1:1000 dilution, and mouse monoclonal anti-Actin antibodies at a 1:2000 dilution) overnight at 4 °C. Primary antibodies were labeled with goat anti-mouse immunoglobulin G (IgG) at a 1:5000 dilution or goat anti-rabbit IgG at a 1:3000 dilution conjugated with horseradish peroxidase (Pierce) and shocked on a shaking table for 1 h at RT. Immunoreactive bands were de-

ected by incubation of the membranes with enhanced chemiluminescence (ECL) reagents.

Measurement of the mitochondrial membrane potential ($\Delta\Psi_m$): The mitochondrial membrane potential ($\Delta\Psi_m$) was monitored by using the fluorescent dye Rh123. Rh123 was added at a final concentration of 1 μM for 30 min at 37 °C after HL-60 cells had been treated with drugs at various concentrations and washed with PBS. Cells were collected and washed twice with PBS. Fluorescence was performed on a FACScaria flow cytometer by using the FL1 channel (fluorescein isothiocyanate (FITC) channel).

Western blot detection of cytochrome c release: Mitochondria were freshly isolated from normal HL-60 cells. Briefly, cells (3×10^7) were harvested and washed in ice-cold PBS for each mitochondria isolation experiment, which was performed by using the Pierce Mitochondria Isolation Kit (Pierce, Rockford, IL, USA) or the Dounce homogenization method. Aliquots of the mitochondrial preparation were incubated with ABT-737 at 2 μM or tested compounds at 5 μM , respectively, at 37 °C for 30 min. After centrifugation at 12000 g for 5 min, the supernatants were analyzed for the presence of cytochrome c by western blotting. Mitochondrial pellets were resuspended in lysis buffer and were also analyzed by western blotting.

Reagents and material: The Alexa Fluor 488 Annexin V/Dead Cell Apoptosis Kit and MitoSOX Red mitochondrial superoxide indicator (MitoSOX) were purchased from Molecular Probes (Eugene, OR, USA). Anti-cytochrome c monoclonal antibody (mAb) and anti-actin mAb were purchased from Santa Cruz Biotechnology (Santa Cruz, CA, USA). Antiporin mAb was purchased from MitoSciences (Eugene, OR, USA). Caspase-9 mouse mAb and PARP rabbit mAb were purchased from Cell Signaling Technology (CST; MA, USA). Rhodamine 123 (Rh123), trypsin, and sodium succinate were purchased from Sigma (St. Louis, MO, USA). Unless stated otherwise, other reagents used in this study were of analytical purity and obtained from Sinopharm Chemical Reagent Co., Ltd. (Shanghai, P. R. China). Mitochondrial buffer (MT buffer) containing 250 mM sucrose, 10 mM 2-[4-(2-hydroxyethyl)-1-piperazinyl]ethanesulfonic acid (HEPES), 1 mM ethylene glycol tetraacetic acid (EGTA), 4.2 mM sodium succinate, and 1 mM potassium dihydrogen phosphate and adjusted to pH 7.0 with 1 M potassium hydroxide, was used for mitochondrial washing and staining. All of the buffers were filtered through a 0.22 μm filter and used within three weeks.

Supporting Information

The Supporting Information contains additional results of ^{15}N -HSQC spectroscopy, molecular modeling, and apoptotic mechanism studies. Furthermore, protocols for the chemical synthesis or intermediary compounds, along with characterization data for all compounds, and more details of the FP-based binding assay are also given in the Supporting Information.

Acknowledgements

The authors are grateful for financial support from the Chinese National Natural Science Foundation (grants no. 81172984, 21072213, 21002117, 21102168, 21102165, and 20921091) and the 863 High-Tech program from the Chinese Ministry of Science and Technology (grant no. 2012AA020308).

Keywords: antitumor agents • apoptosis • Bcl-2 family proteins • inhibitors • lead optimization • protein–protein interactions

- [1] J. C. Reed, *Nat. Rev. Drug Discovery* **2002**, *1*, 111–121.
- [2] S. W. Fesik, *Nat. Rev. Cancer* **2005**, *5*, 876–885.
- [3] M. H. Andersen, J. C. Becker, P. Straten, *Nat. Rev. Drug Discovery* **2005**, *4*, 399–409.
- [4] A. Vazquez, E. E. Bond, A. J. Levine, G. L. Bond, *Nat. Rev. Drug Discovery* **2008**, *7*, 979–987.
- [5] T. G. Cotter, *Nat. Rev. Cancer* **2009**, *9*, 501–507.
- [6] S. Cory, J. M. Adams, *Nat. Rev. Cancer* **2002**, *2*, 647–656.
- [7] G. Lessene, P. E. Czabotar, P. M. Colman, *Nat. Rev. Drug Discovery* **2008**, *7*, 989–1000.
- [8] A. Ashkenazi, *Nat. Rev. Drug Discovery* **2008**, *7*, 1001–1012.
- [9] M. R. Arkin, J. A. Wells, *Nat. Rev. Drug Discovery* **2004**, *3*, 301–317.
- [10] L. Zhao, J. Chmielewski, *Curr. Opin. Struct. Biol.* **2005**, *15*, 31–34.
- [11] J. A. Wells, C. L. McClendon, *Nature* **2007**, *450*, 1001–1009.
- [12] T. Oltersdorf, S. W. Elmore, A. R. Shoemaker, R. C. Armstrong, D. J. Augeri, B. A. Belli, M. Bruncko, T. L. Deckwerth, J. Dinges, P. J. Hajduk, M. K. Joseph, S. Kitada, S. J. Korsmeyer, A. R. Kunzer, A. Letai, C. Li, M. J. Mitten, D. G. Nettesheim, S. Ng, P. M. Nimmer, J. M. O'Connor, A. Oleksijew, A. M. Petros, J. C. Reed, W. Shen, S. K. Tahir, C. B. Thompson, K. J. Tomaselli, B. Wang, M. D. Wendt, H. Zhang, S. W. Fesik, S. H. Rosenberg, *Nature* **2005**, *435*, 677–681.
- [13] C. M. Park, M. Bruncko, J. Adickes, J. Bauch, H. Ding, A. Kunzer, K. C. Marsh, P. Nimmer, A. R. Shoemaker, X. Song, S. K. Tahir, C. Tse, X. Wang, M. D. Wendt, X. Yang, H. Zhang, S. W. Fesik, S. H. Rosenberg, S. W. Elmore, *J. Med. Chem.* **2008**, *51*, 6902–6915.
- [14] C. Tse, A. R. Shoemaker, J. Adickes, M. G. Anderson, J. Chen, S. Jin, E. F. Johnson, K. C. Marsh, M. J. Mitten, P. Nimmer, L. Roberts, S. K. Tahir, Y. Xiao, X. Yang, H. Zhang, S. Fesik, S. H. Rosenberg, S. W. Elmore, *Cancer Res.* **2008**, *68*, 3421–3428.
- [15] S. Kitada, M. Leone, S. Sareth, D. Zhai, J. C. Reed, M. Pellecchia, *J. Med. Chem.* **2003**, *46*, 4259–4264.
- [16] B. Becattini, S. Kitada, M. Leone, E. Monosov, S. Chandler, D. Zhai, T. J. Kipps, J. C. Reed, M. Pellecchia, *Chem. Biol.* **2004**, *11*, 389–395.
- [17] M. Nguyen, R. C. Marcellus, A. Roulston, M. Watson, L. Serfass, S. R. Murthy Madiraju, D. Goulet, J. Viallet, L. Belec, X. Billot, S. Acoca, E. Purisima, A. Wiegmanns, L. Cluse, R. W. Johnstone, P. Beauparlant, G. C. Shore, *Proc. Natl. Acad. Sci. USA* **2007**, *104*, 19512–19517.
- [18] J. L. Wang, D. Liu, Z. J. Zhang, S. Shan, X. Han, S. M. Srinivasula, C. M. Croce, E. S. Alnemri, Z. Huang, *Proc. Natl. Acad. Sci. USA* **2000**, *97*, 7124–7129.
- [19] A. Degterev, A. Lugovskoy, M. Cardone, B. Mulley, G. Wagner, T. Mitchison, J. Yuan, *Nat. Cell Biol.* **2001**, *3*, 173–182.
- [20] G. Wang, Z. Nikolovska-Coleska, C. Y. Yang, R. Wang, G. Tang, J. Guo, S. Shangary, S. Qiu, W. Gao, D. Yang, J. Meagher, J. Stuckey, K. Krajewski, S. Jiang, P. P. Roller, H. O. Abaan, Y. Tomita, S. Wang, *J. Med. Chem.* **2006**, *49*, 6139–6142.
- [21] G. Tang, Z. Nikolovska-Coleska, S. Qiu, C. Y. Yang, J. Guo, S. Wang, *J. Med. Chem.* **2008**, *51*, 717–720.
- [22] L. Wang, D. T. Sloper, S. N. Addo, D. Tian, J. W. Slaton, C. Xing, *Cancer Res.* **2008**, *68*, 4377–4383.
- [23] J. Wei, S. Kitada, M. F. Rega, J. L. Stebbins, D. Zhai, J. Cellitti, H. Yuan, A. Emdadi, R. Dahl, Z. Zhang, L. Yang, J. C. Reed, M. Pellecchia, *J. Med. Chem.* **2009**, *52*, 4511–4523.
- [24] J. Wei, J. L. Stebbins, S. Kitada, R. Dash, W. Placzek, M. F. Rega, B. Wu, J. Cellitti, D. Zhai, L. Yang, R. Dahl, P. B. Fisher, J. C. Reed, M. Pellecchia, *J. Med. Chem.* **2010**, *53*, 4166–4176.
- [25] Y. Feng, X. Ding, T. Chen, L. Chen, F. Liu, X. Jia, X. Luo, X. Shen, K. Chen, H. Jiang, H. Wang, H. Liu, D. Liu, *J. Med. Chem.* **2010**, *53*, 3465–3479.
- [26] Z. Zhang, G. Wu, F. Xie, T. Song, X. Chang, *J. Med. Chem.* **2011**, *54*, 1101–1105.
- [27] B. E. Sleebs, P. E. Czabotar, W. J. Fairbrother, W. D. Fairlie, J. A. Flygare, D. Huang, W. J. A. Kersten, M. F. T. Koehler, G. Lessene, K. Lowes, J. P. Pariset, B. J. Smith, M. L. Smith, A. J. Souers, I. P. Street, H. Yang, J. B. Baell, *J. Med. Chem.* **2011**, *54*, 1914–1926.

- [28] H. Zhou, A. Aguilar, J. Chen, L. Bai, L. Liu, J. L. Meagher, C. Y. Yang, D. McEachern, X. Cong, J. A. Stuckey, S. Wang, *J. Med. Chem.* **2012**, *55*, 6149–6161.
- [29] J. Chen, H. Zhou, A. Aguilar, L. Liu, L. Bai, D. McEachern, C. Y. Yang, J. L. Meagher, J. A. Stuckey, S. Wang, *J. Med. Chem.* **2012**, *55*, 8502–8514.
- [30] A. J. Souers, J. D. Levenson, E. R. Boghaert, S. L. Ackler, N. D. Catron, J. Chen, B. D. Dayton, H. Ding, S. H. Enschede, W. J. Fairbrother, D. C. Huang, S. G. Hymowitz, S. Jin, S. L. Khaw, P. J. Kovar, L. T. Lam, J. Lee, H. L. Maecker, K. C. Marsh, K. D. Mason, M. J. Mitten, P. M. Nimmer, A. Oleksijew, C. H. Park, C. M. Park, D. C. Phillips, A. W. Roberts, D. Sampath, J. F. Seymour, M. L. Smith, G. M. Sullivan, S. K. Tahir, C. Tse, M. D. Wendt, Y. Xiao, J. C. Xue, H. Zhang, R. A. Humerickhouse, S. H. Rosenberg, S. W. Elmore, *Nat. Med.* **2013**, *19*, 202–208.
- [31] A. Friberg, D. Vigil, B. Zhao, R. N. Daniels, J. P. Burke, P. M. Garcia-Barantes, D. Camper, B. A. Chauder, T. Lee, E. T. Olejniczak, S. W. Fesik, *J. Med. Chem.* **2013**, *56*, 15–30.
- [32] A. Aguilar, H. Zhou, J. Chen, L. Liu, L. Bai, D. McEachern, C. Y. Yang, J. Meagher, J. Stuckey, S. Wang, *J. Med. Chem.* **2013**, *56*, 3048–3067.
- [33] G. Lessene, P. E. Czabotar, B. E. Sleeb, K. Zobel, K. N. Lowes, J. M. Adams, J. B. Baell, P. M. Colman, K. Deshayes, W. J. Fairbrother, J. A. Flygare, P. Gibbons, W. J. A. Kersten, S. Kulasegaram, R. M. Moss, J. P. Parisot, B. J. Smith, I. P. Street, H. Yang, D. C. S. Huang, K. G. Watson, *Nat. Chem. Biol.* **2013**, *9*, 390–397.
- [34] Y. Tanaka, K. Aikawa, G. Nishida, M. Homma, S. Sogabe, S. Igaki, Y. Hayano, T. Sameshima, I. Miyahisa, T. Kawamoto, M. Tawada, Y. Imai, M. Inazuka, N. Cho, Y. Imaeda, T. Ishikawa, *J. Med. Chem.* **2013**, *56*, 9635–9645.
- [35] L. Han, R. Wang, *ChemMedChem* **2013**, *8*, 1437–1440.
- [36] R. J. Youle, A. Strasser, *Nat. Rev. Mol. Cell Biol.* **2008**, *9*, 47–59.
- [37] M. Konopleva, R. Contractor, T. Tsao, I. Samudio, P. P. Ruvolo, S. Kitada, X. Deng, D. Zhai, Y. X. Shi, T. Sneed, M. Verhaegen, M. Soengas, V. R. Ruvolo, T. McQueen, W. D. Schober, J. C. Watt, T. Jiffar, X. Ling, F. C. Marini, D. Harris, M. Dietrich, Z. Estrov, J. McCubrey, W. S. May, J. C. Reed, M. Andreeff, *Cancer Cell* **2006**, *10*, 375–388.
- [38] M. F. van Delft, A. H. Wei, K. D. Mason, C. J. Vandenberg, L. Chen, P. E. Czabotar, S. N. Willis, C. L. Scott, C. L. Day, S. Cory, J. M. Adams, A. W. Roberts, D. C. Huang, *Cancer Cell* **2006**, *10*, 389–399.
- [39] C. Skoda, B. M. Erovic, V. Wachek, L. Vormittag, F. Wrba, H. Martinek, G. Heiduschka, P. Kloimstein, E. Selzer, D. Thurnher, *Oncol. Rep.* **2008**, *19*, 1499–1503.
- [40] B. Zhou, X. Li, Y. Li, Y. Xu, Z. Zhang, M. Zhou, X. Zhang, Z. Liu, J. Zhou, C. Cao, B. Yu, R. Wang, *ChemMedChem* **2011**, *6*, 904–921.
- [41] Y. Xu, M. Zhou, Y. Li, C. Li, Z. Zhang, B. Yu, R. Wang, *ChemMedChem* **2013**, *8*, 1345–1352.
- [42] X. Ding, Y. Li, L. Lv, M. Zhou, L. Han, Z. Zhang, Q. Ba, J. Li, H. Wang, H. Liu, R. Wang, *ChemMedChem* **2013**, *8*, 1986–2014.
- [43] H. C. Kolb, M. G. Finn, K. B. Sharpless, *Angew. Chem.* **2001**, *113*, 2056–2075; *Angew. Chem. Int. Ed.* **2001**, *40*, 2004–2021.
- [44] Z. Nikolovska-Coleska, R. Wang, X. Fang, H. Pan, Y. Tomita, P. Li, P. P. Roller, K. Krajewski, N. G. Saito, J. A. Stuckey, S. Wang, *Anal. Biochem.* **2004**, *332*, 261–273.
- [45] S. W. Muchmore, M. Sattler, H. Liang, R. P. Meadows, J. E. Harlan, H. S. Yoon, D. Nettesheim, B. S. Chang, C. B. Thompson, S. L. Wong, S. L. Ng, S. W. Fesik, *Nature* **1996**, *381*, 335–341.
- [46] P. E. Czabotar, E. F. Lee, M. F. van Delft, C. L. Day, B. J. Smith, D. C. Huang, W. D. Fairlie, M. G. Hinds, P. M. Colman, *Proc. Natl. Acad. Sci. USA* **2007**, *104*, 6217–6222.

Received: January 25, 2014

Published online on April 29, 2014